DETERMINATION OF BULK PERMEABILITY WITHIN THE MORIEN GROUP USING THE FORCING OF OCEAN TIDES IN THE SYDNEY BASIN IN CAPE BRETON, NOVA SCOTIA

Kevin Joseph Doyle

Submitted in Partial Fulfilment of the Requirements
for the Degree of Bachelor of Sciences
Department of Earth Sciences
Dalhousie University, Halifax, Nova Scotia
March 1997

Distribution License

DalSpace requires agreement to this non-exclusive distribution license before your item can appear on DalSpace.

NON-EXCLUSIVE DISTRIBUTION LICENSE

You (the author(s) or copyright owner) grant to Dalhousie University the non-exclusive right to reproduce and distribute your submission worldwide in any medium.

You agree that Dalhousie University may, without changing the content, reformat the submission for the purpose of preservation.

You also agree that Dalhousie University may keep more than one copy of this submission for purposes of security, back-up and preservation.

You agree that the submission is your original work, and that you have the right to grant the rights contained in this license. You also agree that your submission does not, to the best of your knowledge, infringe upon anyone's copyright.

If the submission contains material for which you do not hold copyright, you agree that you have obtained the unrestricted permission of the copyright owner to grant Dalhousie University the rights required by this license, and that such third-party owned material is clearly identified and acknowledged within the text or content of the submission.

If the submission is based upon work that has been sponsored or supported by an agency or organization other than Dalhousie University, you assert that you have fulfilled any right of review or other obligations required by such contract or agreement.

Dalhousie University will clearly identify your name(s) as the author(s) or owner(s) of the submission, and will not make any alteration to the content of the files that you have submitted.

If you have questions regarding this license please contact the repository manager at dalspace@dal.ca.

Grant the distribution license by signing and dating below.

_____ _____

Name of signatory Date

Dalhousie University

Department of Earth Sciences
Halifax, Nova Scotia
Canada B3H 3J5
(902) 494-2358
FAX (902) 494-6889

DATE April 15, 1997

AUTHOR Kevin Joseph Doyle

TITLE DETERMINATION OF BULK PERMEABILITY WITHIN THE MORIEN GROUP USING THE FORCING OF OCEAN TIDES IN THE SYDNEY BASIN IN CAPE BRETON, NOVA SCOTIA

Degree BSc Convocation October Year 1997

Abstract

Since November 1992 the Lingan Colliery in the Sydney coalfield has been steadily filling with water. At the same time the water level in the previously flooded 1B region and the No 26 Colliery has been gradually decreasing. There are no direct excavated links between the Lingan and No.26 Collieries. It is believed that influences of the longwall mining in the Phalen Colliery have caused damage to the barrier pillar between the Lingan and No 26 Collieries, resulting in a hydrological connection.
The water levels in the workings in question have been monitored and recorded by the Cape Breton Development Corporation (CBDC) since 1986, but after the 1992 massive inrush the monitoring system was upgraded to provide a more complete picture of what is happening within the mine with respect to mine waters. In Lingan, water level data recorded by CBDC, show a strong tidal signal that overprints the increasing water level signal in the mine. Comparison with regional tidal records over the same time period has confirmed this correlation between water level data and the tidal signal. The differences found in the correlations will be used to determining the bulk permeability of the strata from the Harbour coal seam to the seafloor.
An analysis of the phase shift and amplitude of the tidal signal in the water level records provides a direct estimate of formation permeability, based on Darcy's law and assuming that there is laminar flow through out the formation. Water level data, analyzed to remove the longer time period fluctuations in levels, are presented with tidal data. The bulk permeability based on the tidal signal differences are found to fall within the silt to sand range (10^{-2} to 10^{-3} cm/sec).

Key Words: bulk permeability, hydrological connection, correlation, Darcy's law, laminar flow, Colliery, phase shift, amplitude shift

Table of Contents

TABLE OF FIGURES

TABLE OF TABLES

TABLE OF ABBREVIATIONS AND SYMBOLS

CBDC .....Cape Breton Development Corporation

LPM.....liters per minute

gpm.....gallons per minute

mD .....millidarcies

cm .....centimeters

sec.....seconds

v .....velocity

K .....hydraulic conductivity

k ..... intrinsic permeability

ρ .....density of the fluid

μ .....viscosity of the fluid

g .....Gravitational attraction

A .....cross-sectional area

h .....energy or head loss

q .....flow rate

i, $\Delta h/l$ .....hydraulic gradient

x .....distance

t .....time

ACKNOWLEDGMENTS

I would like to thank Dr. Kate Moran for making this project happen. I have never met anyone before who has the enthusiasm and drive that Kate has when it comes to their job and their life. Without your willingness to teach and ensure that I used the knowledge that I have to the best of my ability, Kate, I highly doubt that I would have made it.

I also extend appreciation to the Cape Breton Development Corporation, Phalen Colliery for allowing me to use their data and to their staff for taking the time to help me. Mr. Gary Ellerbrok's knowledge of the Collieries and desire to understand the aspects of this project was an invaluable resource and at times a relief because I couldn't find anyone who knew the answers to my little questions. Without your explanations Gary I would probably still be in the dark. Thanks.

I would also like to thank Dr. Martin Gibling and Dr. Tom Martel for giving me the opportunity to do this interesting project as my thesis project.

The list of friends that I would like to thank would probably take up half of this thesis so I will just say that I know who you are and I owe you one. But I must thank Lucy and Askja for their ability to always make things seem fine when there was no end in sight.....

To all of you who have supported me for the last four years, especially Mom and Dad, I thank you.

CHAPTER 1 INTRODUCTION

1.1 Introduction

Since November of 1992 the Lingan coal mine workings, located in the Sydney region of Cape Breton Island, Nova Scotia (Figure 1.1), have been filling with water that originated in other flooded mines in the region. The Lingan mine is part of a complex fluid regime that involves several mines that are interconnected in a variety of ways, either through ventilation systems or hydrologic connections, to form a hydraulic system (Figure 1.2). This study examines the changes in water levels in the collieries, with the aim of using these data to estimate the bulk permeability of the overlying rock mass. The mine is owned and operated by the Cape Breton Development Corporation, CBDC, a crown corporation based in the Sydney area. Mine plans are shown in Figure 1.3. This study is concerned only with the Lingan, No.26, 1B and Phalen Collieries.

This thesis is concerned specifically with the hydraulic regime that is supplying the water that flows into the Lingan Colliery. In 1992, when the water level began to lower in the 1B Colliery, there was a severe inrush of water into Lingan. A barrier pillar between the No.26 and Lingan, which formed a hydrologic connection between the two Collieries, had been breached. The 1B Colliery was abandoned in 1985 due to a mine fire. As a direct result of the fire, pumping of this mine ceased which resulted in the filling of No.26. Lingan and No.26 are both in the Harbour seam. These adjacent collieries are approximately 305 meters apart (Figure 1.4) . The No.26 Colliery, which in turn is hydrologically connected to the 1B colliery, began to release water into Lingan

Study Area Location Map

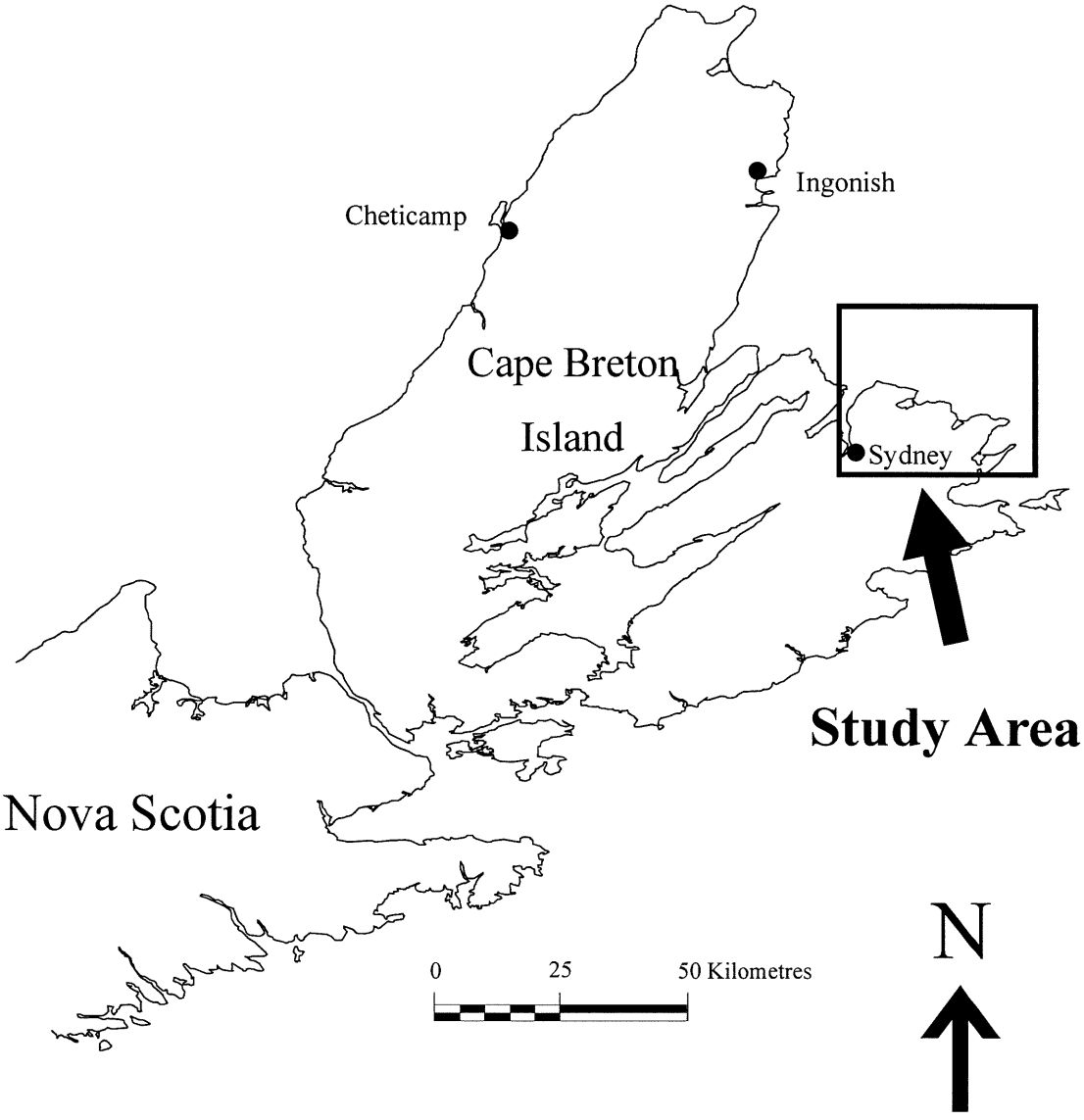

Figure 1. Location of CBDC mines in North Eastern Cape Breton, Nova Scotia.

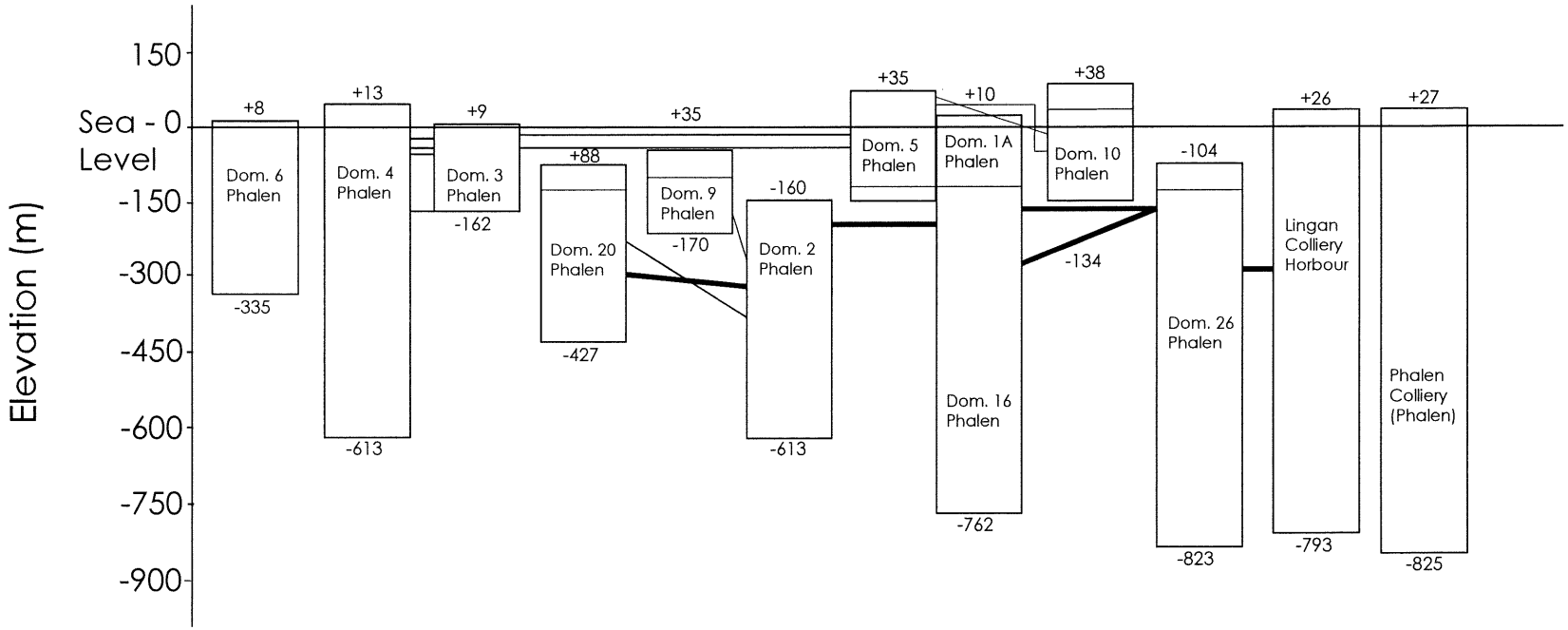

Figure 1.2 Cross section showing the depth of mine colleries (redrawn from Cape Breton Development Corporation, 1994). All elevations are in meters.

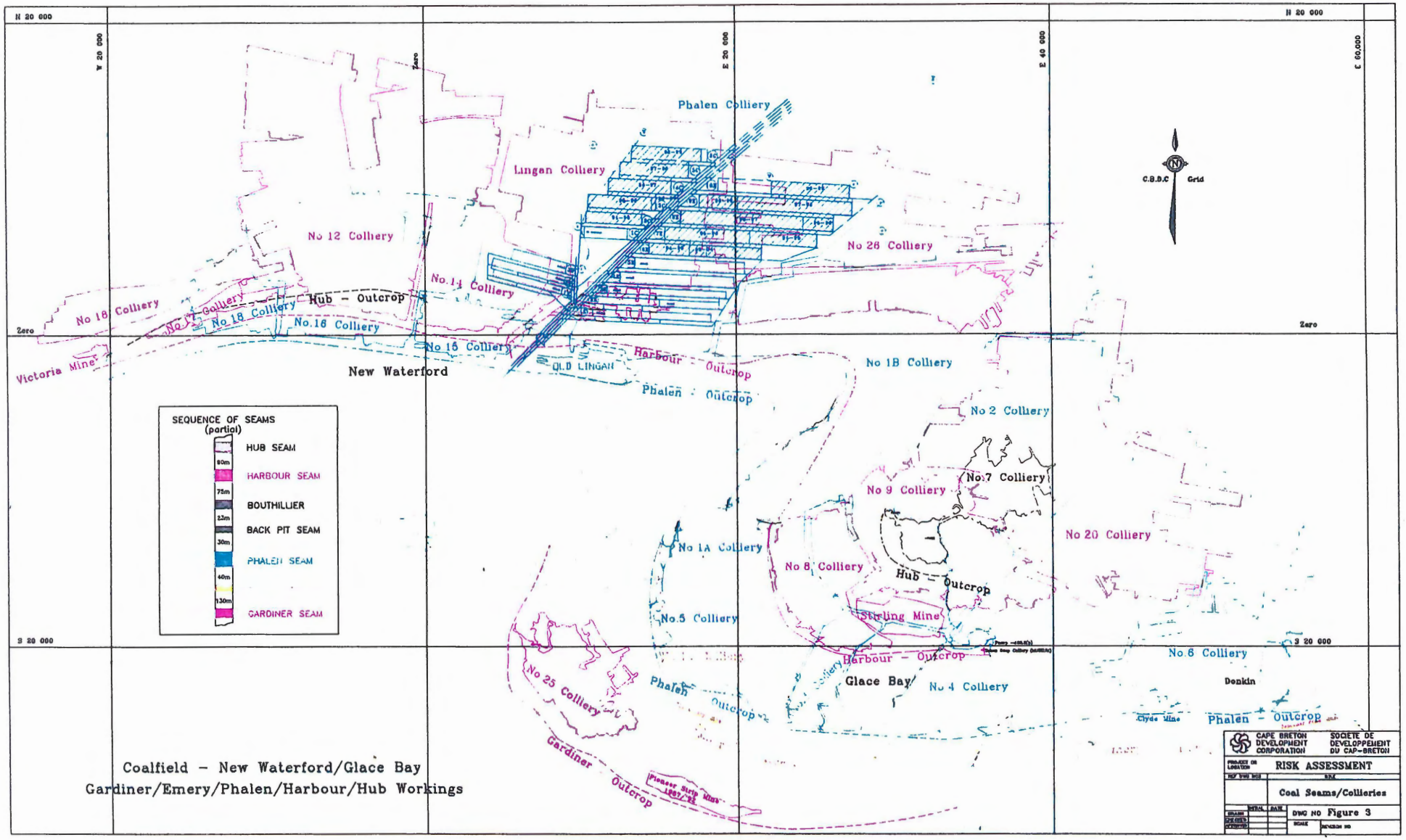

Figure 1.3 Map showing the CBDC Collieries in the Sydney coalfield (CBDC, 1994).

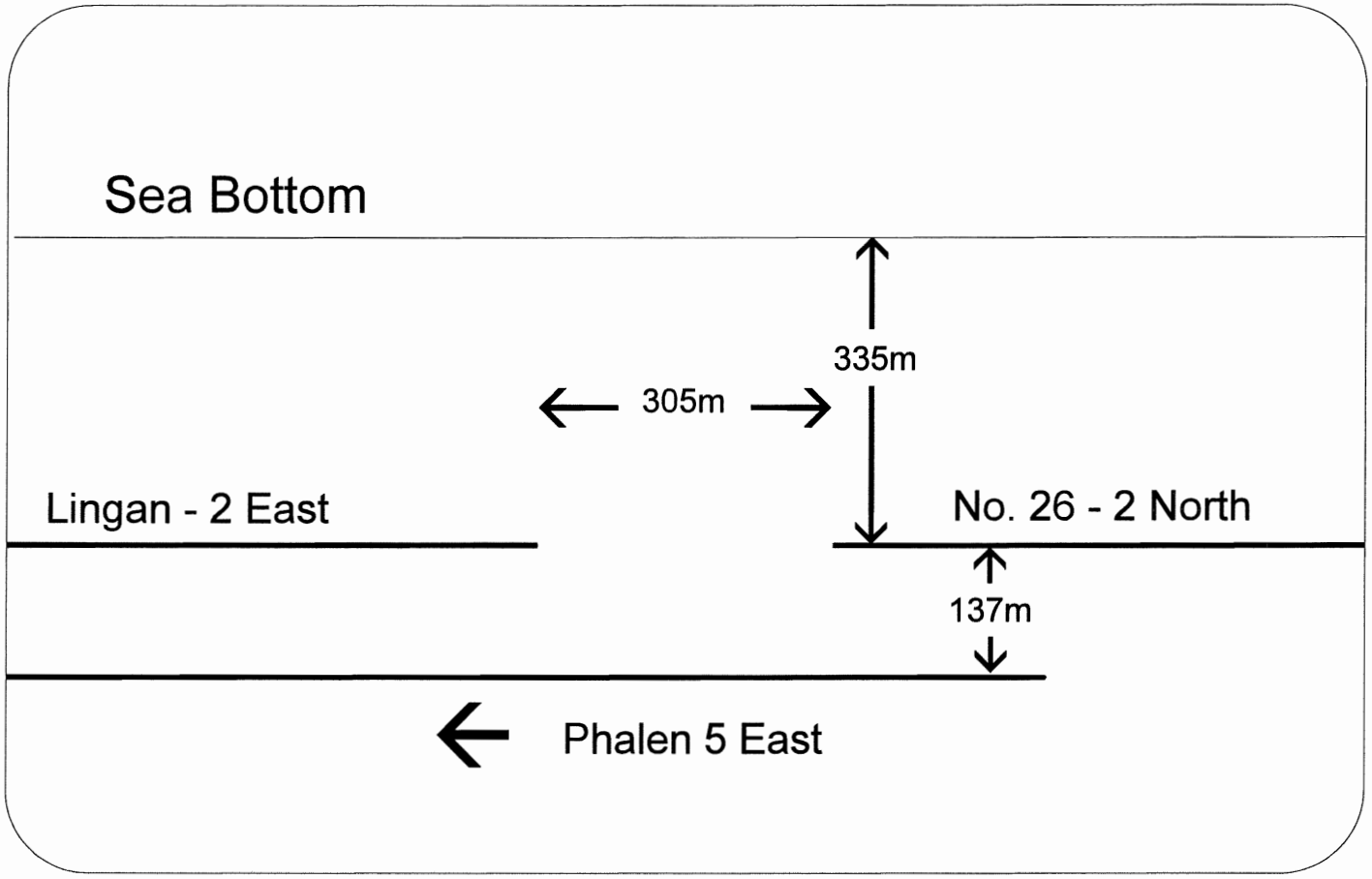

Figure 1.4 Relationship of Lingan, No.26 and the Phalen Collieries (Redrawn from Cain *et. al.,* 1994).

in 1992. It is thought that the introduction of mine water through No.26 into Lingan was due to a structural failure between the two mines. This failure was due directly to mining operations that were underway in the deeper Phalen workings, some of which are located directly underneath the Lingan and No.26 workings.

The Lingan colliery cannot be operated under present conditions because of difficulty to control the flooding. The initial flow rate of water in 1992, into Lingan reached a maximum of approximately 18000 liters per minute (Lpm) into the Lingan 2 east panel (CBDC, 1994) (Figure 1.5). The rate of flooding has been decreasing steadily since 1993, with flow rates reaching as low as 200 to 500 Lpm. The steady decrease of fluid movement can be attributed to the fact that, at the initial break, the water column in No.26 was at approximately 305 meters; now it is at approximately 30 meters, which represents a drastic loss in potential energy from the source body of water for the Lingan inrush (Gary Ellerbrok, pers. comm., 1997). After abandonment of the Lingan Colliery it was determined that the mine waters could not be removed from the workings without significant treatment and cost to the CBDC.

After the 1992 water inrush into Lingan, the CBDC upgraded its monitoring systems in these mines to establish a more extensive database. Since 1986, water levels in some of the CBDC mines have been monitored. The new system is more accurate and covers a broader area for better definition of the local hydraulic regimes. Since 1993, the water level data from the Lingan Colliery has shown a distinctive sinusoidal signal, which

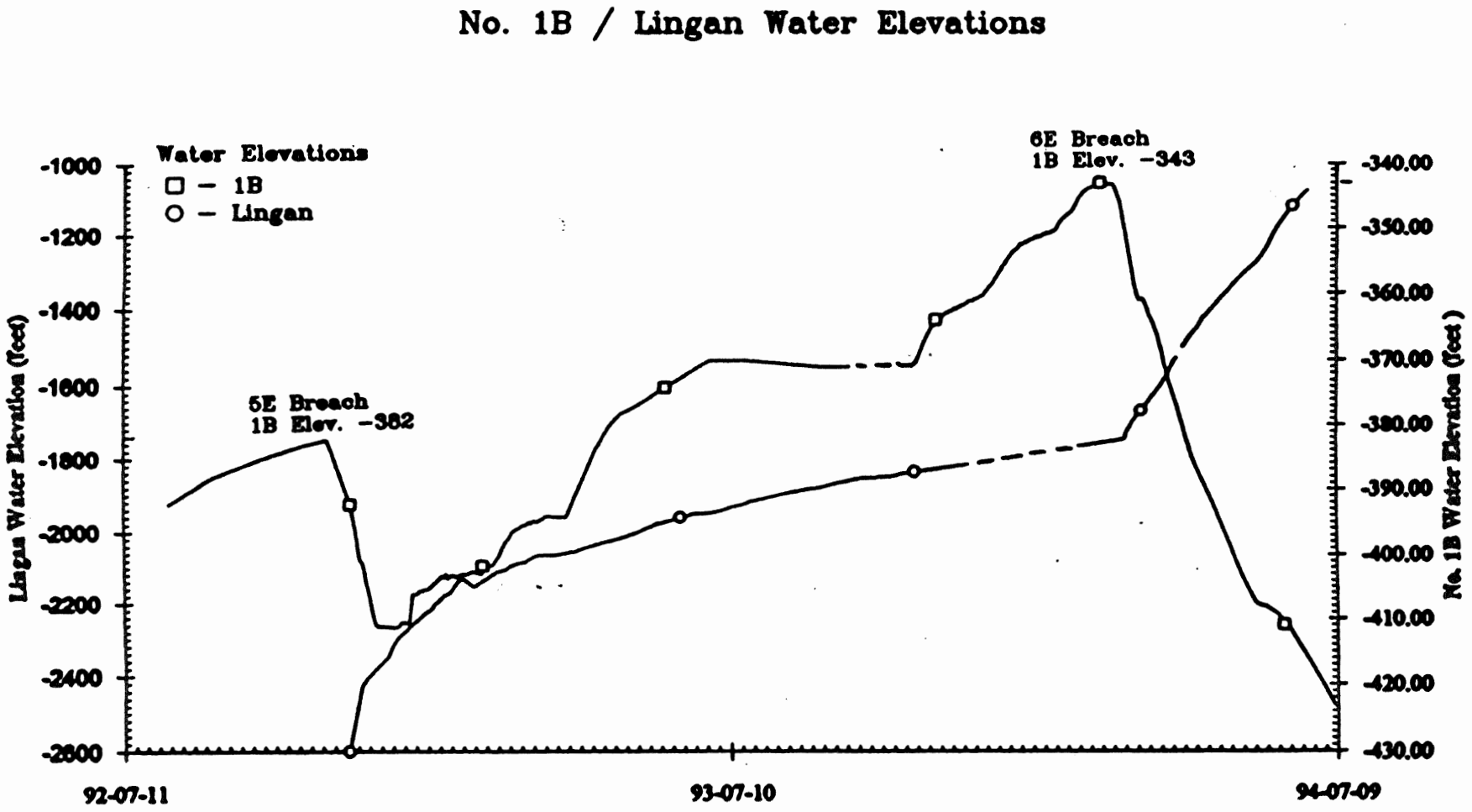

Figure 1.5 Graph showing the water level changes in Lingan and No.1B. First major chance occurred in November 1992 and the second change was in February 1994 (CBDC, 1994).

suggests that external forces influence the waters in the Lingan Colliery. Due to the location of the Lingan workings beneath the seafloor, and the similarity of the sinusoidal wave pattern found in the Lingan water level data with that of the local tidal effect, it is hypothesized that the sinusoidal wave is generated by tidal activity.

1.2 Objectives

The purpose of this project is to determine the bulk permeability of the rock units overlying the Lingan coal mine workings through the use of ocean tides and mine water level data. Bulk permeability on the formation scale is a useful tool in determining flow regimes and characteristics of rocks, such as the total transmissivity. The bulk permeability will be determined using the hypothesis proposed by Van der Kamp and Gale (1983), which states that the permeability of a subsea geological unit can be determined through the integration of hydraulic head readings and the tidal elevations of the local influencing body of water. In this study, the mine water levels will provide a form of hydraulic head reading; the local influencing tidal body of water is the Atlantic Ocean.

The geology of the study area within the Sydney Basin (discussed in chapter 2) meets the general requirements for the three dimensional equations for stress, strain, and pore pressure in a homogeneous porous medium as defined by Van der Kamp and Gale (1983). Variations in pore pressure and stress imposed on the affected rock by tidal

fluctuations are related to its permeability, and will lead to a time lag between tidal readings and the Lingan mine water level fluctuations. The correlation of phase and amplitude shifts are used for calculating the bulk permeability of the overlying rock, which extends from the ocean floor to the mine workings.

The relationship between the determined bulk permeability of the units overlying the Lingan Colliery and the permeabilities of similar rock units measured in the lab are used to observe how changes in the *in situ* rock, such as those due to subsidence following mining, are causing changes in the permeability of overlying strata at the Lingan Colliery.

1.3 Colliery Influences

Several factors influence the hydrologic systems of the Lingan, 1B, No.26 and Phalen workings from the view point of physical properties. These factors include the compressibility and permeability of the units above the workings, and the redistribution of rock load as operations in the Phalen mine continues to remove sections of the Phalen coal seam that underlies the Lingan Colliery. It is operating in the deeper Phalen mine that has led to the physical changes in the upper rocks (Reddish *et.* al., 1994).

Within the study area mining causes local redistribution of stress in the surrounding strata, on the individual pore spaces, and on the units of the Morien Group. The magnitude of stress changes at a range of scales, from micrometers to meters, causes overall changes in the *in situ* permeability which , in turn, influences the migration of water and/or gases through the pore spaces. A cross section of the study area that show

the distances that the seams extend from the shore out under the ocean and the depth in the Sydney Basin at which the mines are located are shown in Figure 1.6.

At present, the greatest influence on the environment in the Lingan workings is the change in seepage pressure is reflected in the subsequent change in water found within the workings. In this special situation, the transient loading that is being imposed within the seafloor sediments by ocean tides provides a means measuring the magnitude of tidal influences on pressure with depth in a saturated medium (MacKillop, 1994).

The analysis of bulk permeability is treated here as a two dimensional problem, in the horizontal and vertical. Tidally-induced pressure differences in seafloor formations have been used to determine the compressibility, permeability and gas content on the formation scale in other marine settings (Wang and Davis, 1996). These analyses assumed diffusive propagation of tidal pressure variations between the seafloor and the formation. Although the problem in Lingan is similar to those reported in the other study, in that the driving forces are tides, flow over Lingan is not thought to be purely diffusive. Because water levels change within Lingan and No.26 over tidal cycles, the problem is one of advective flow, providing a direct measurement of hydraulic conductivity.

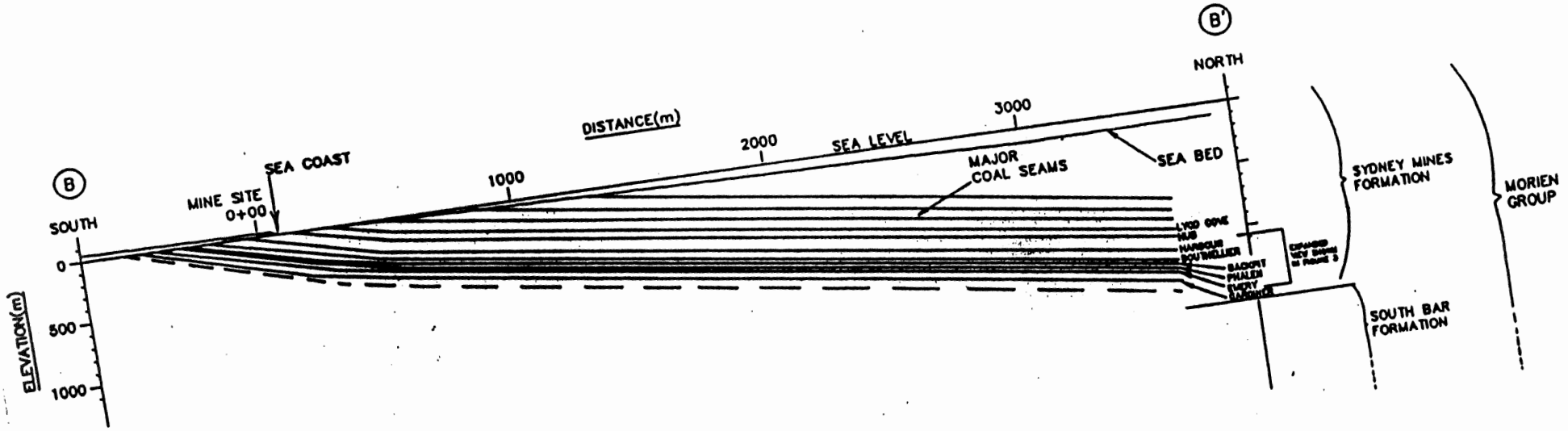

Figure 1.6 Transect in the New Waterford region showing the relationship of the coal seams from the coast of Cape Breton out into the Sydney Basin (CBDC, 1994).

1.3.1 Technique used to Determine Permeability

Using criteria discussed in Chapter 3, the tidal data were scaled within a defined time and elevation above sea level frame. All graphs of the mine water level data are set to the same criteria and parameters but, as will be described later, signals from the mine waters are de-trended so that they are easier to correlate. Once these correlations are made, the differences in signals are used to generate an *in situ* permeability estimate.

CHAPTER 2 REGIONAL GEOLOGY

2.1 Geology of the Sydney Basin

The Sydney Basin is one of a number of Carboniferous basins found on the northeastern coast of North America. The basin extends from the northeastern coast of Cape Breton Island almost to the western shelf of Newfoundland (Figure 2.1). The offshore part of the Sydney Basin is approximately 36,300 km^2 in area (King and Maclean, 1976), with a Carboniferous basin fill thickness of approximately four kilometers (Gibling *et. al.*, 1987). The much smaller onshore and near offshore portion, known as the Sydney coalfield, has an area of about 520 km^2 (Hacquebard, 1983).

The four kilometers of basin strata were deposited over a period of approximately 75 Ma from the early Carboniferous to the Permian (Figure 2.2). The section is composed of two upward fining megasequences dominated by alluvial, lacustrine and marine strata (Gibling *et. al.*, 1987). A hiatus of approximately 22 Ma separates the two sequences. The lower megasequence, which contains the Horton, Windsor and Canso Groups, accumulated over an approximately 27 Ma period (Gibling *et. al.*, 1987), from the early Mississippian to the Namurian (Figure 2.2). The upper megasequence, which contains the Pennsylvanian Morien Group, accumulated approximately over a 25 Ma period (Gibling *et. al.*, 1987). Unnamed redbeds, possibly Permian in age, lie offshore (Hacquebard, 1983).

The Sydney coalfield is located in the southwestern part of the Sydney Basin in the upper megasequence, the Morien Group, which extends onshore on the northeastern coast

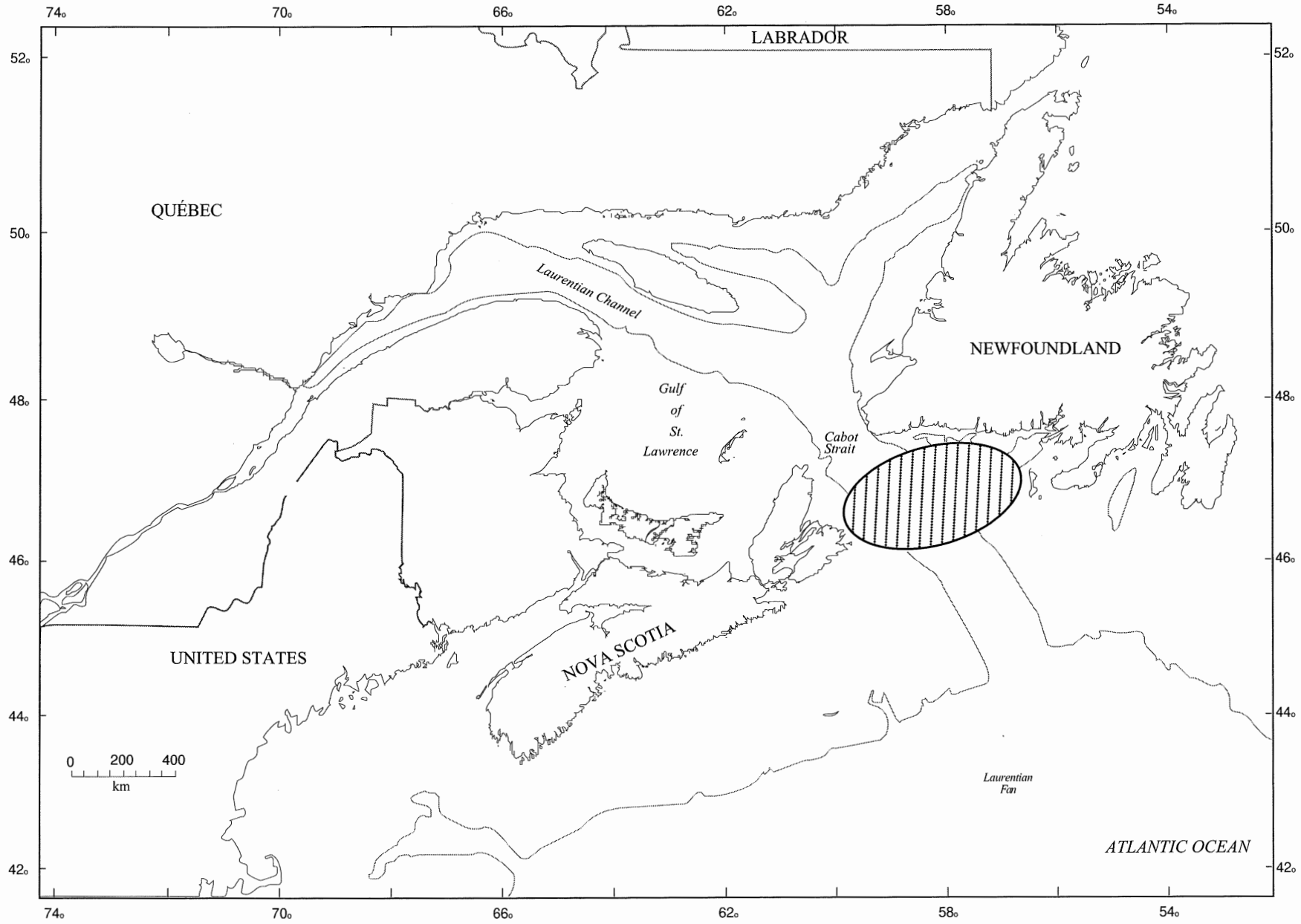

Figure 2.1. Regional map showing the location of the Sydney Basin (hatched area)

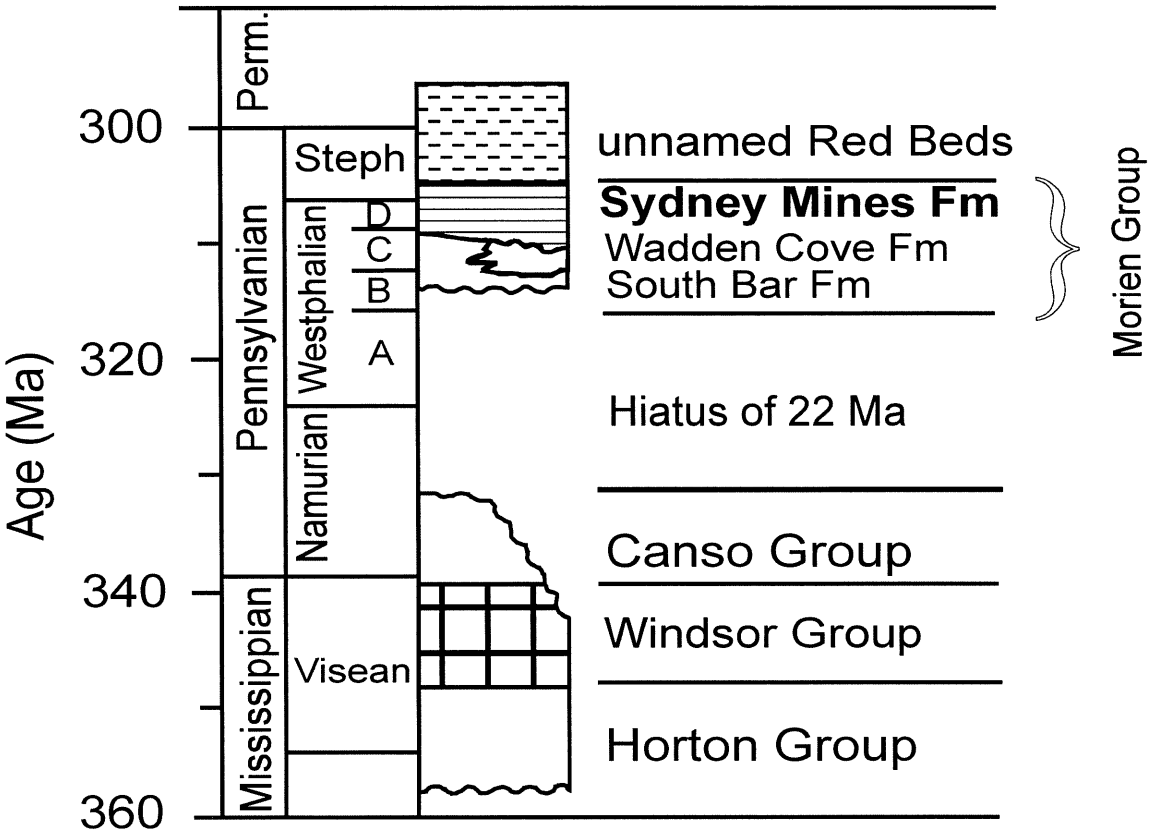

Figure 2.2 Stratigraphic section showing the relationship between the formations.

of Cape Breton. The Morien Group is subdivided into the South Bar, Waddens Cove and Sydney Mines Formations. The maximum onshore thickness of the group is approximately 645 meters in the Glace Bay region (Hacquebard, 1983). The upper portion of the Morien Group, the Sydney Mines Formation, contains economic coal seams that range in age from Westphalian B to Stephanian (Gibling and Bird, 1994). In the offshore, the unnamed redbeds that cover the Sydney Mines Formation range in age from Stephanian probably to early Permian (Gibling *et. al.*, 1987), and are estimated to be 400 meters thick (Hacquebard, 1983).

The Sydney Mines Formation consists of sandstone, mudstone, limestone and coal. The formation is about 500 m in thickness (Gibling and Bird, 1994) with the main constituents being gray and red mudstones, which together forms approximately 50% of the strata. Within this section of strata the formation shows rapid horizontal and vertical variations in layer composition (Gary Ellerbrok, pers. comm., 1997). There is a series of coal seams with thicknesses to a maximum of 4.3 meters occur in the formation (Gibling and Bird, 1994) (Figure 2.3). For the purpose of this study, only the regions of the Harbour and Phalen seams mined in the Phalen and Lingan Collieries are considered.

2.1.1 Structural Geology

Within the Sydney Basin no major faulting has occurred, the basin is, however, fault-bounded by two large scale faults. The Sydney Basin has been described as saucer-shaped due to the gentle dip toward the center of the Sydney Basin (King and MacLean, 1976). The basin is bounded to the northwest by the Mountain Fault and to the

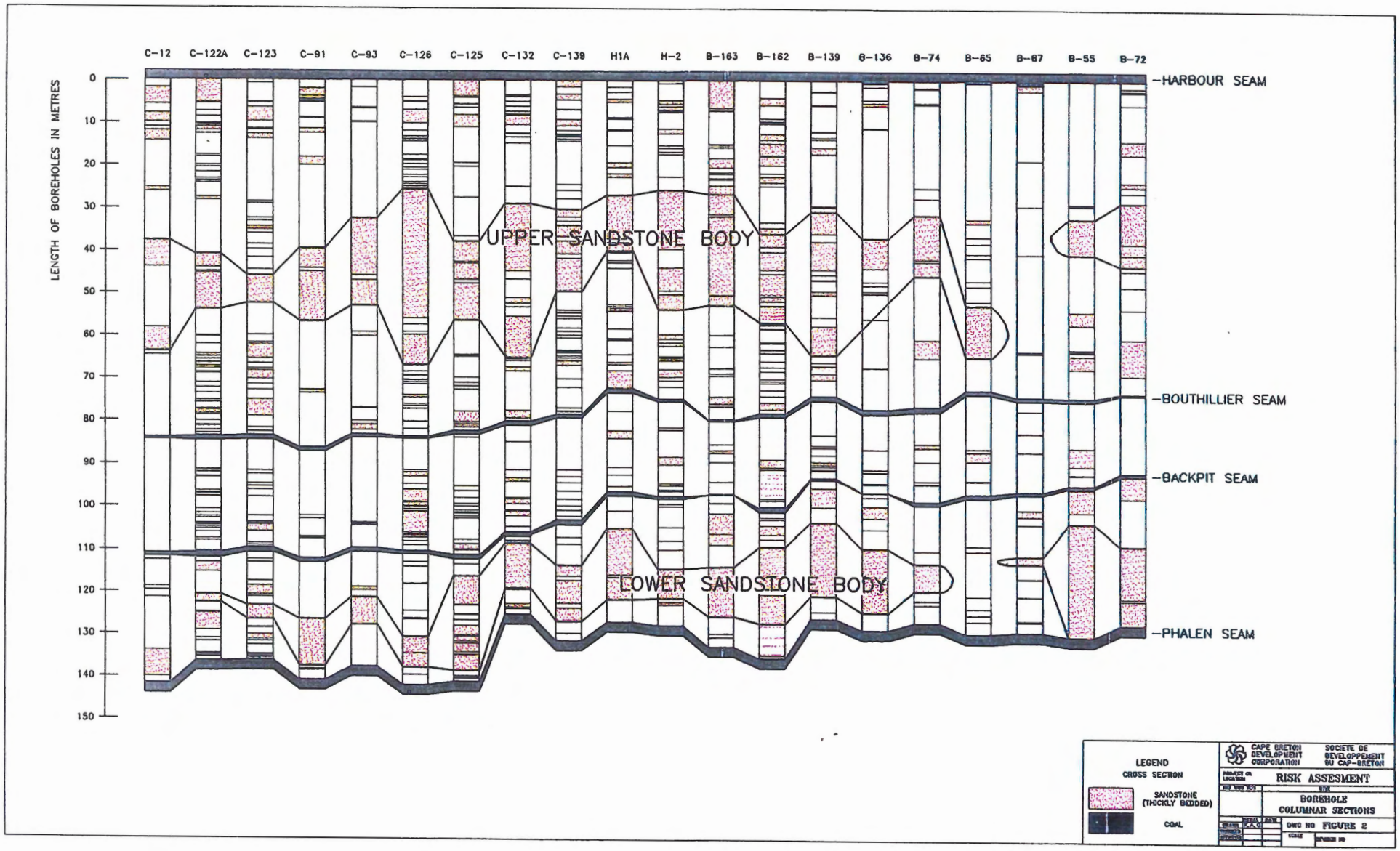

Figure 2.3 Stratigraphic cross section showing the correlations between the Harbour Seam and the Phalen Seam (CBDC, 1994).

southeast by the Mira River-Bateston Fault and is divided into the Ingonish and Glace Bay sub-basins by the Boisdale Anticline.

2.1.2 Coal Geology

Although the Sydney Basin is fault bounded, Gibling *et. al.* (1987) suggest that the structures that affect the coal-bearing strata are the result of differential compaction over fault bounded basement blocks. All the coal seams found in the Morien Group are classified as high volatile "A" bituminous. The Phalen seam, which is stratigraphically deeper than the Harbour Seam, was probably deposited in a fluvially dominated environment, where large amounts of peat accumulated in substantial swamps in a low-gradient alluvial plain (Rust *et. al*, 1987).

CHAPTER 3 WATER LEVEL INFLUENCES

3.1 Introduction

This chapter describes the semi-diurnal to mixed tides that occur in the Sydney Basin. These tides, when related to the water level changes recorded within the workings of the Lingan coal mine, provide a means to calculate the permeability of a near shore section of the Sydney Basin. Water level records from the Lingan workings show an overprinted signal that is very similar to the signal of tidal signal found in the nearby Atlantic Ocean. By correlating the records from the mine with those of a local tidal station at the same scale (centimeters above sea level), and over the same time period, a phase shift and amplitude shift can be measured. These shifts are used to determine the inherent permeability of intervening rock facies. Calculation of this permeability, using phase and amplitude shifts, is discussed in Chapter 4.

3.2 Influence of Ocean Tides

3.2.1 Ocean Tides

A tide is a sinusoidal wave with a crest and a trough that has periodicity, which is the tendency to repeat itself over a regular interval (Dooley, 1995). This occurs at intervals of either 12 hours and 25 minutes or at 24 hours and 50 minutes. When dealing with tides it must be recognized that there are controlling factors such as gravitational attraction and centrifugal force (Figure 3.1). The moon is the main regulator of the

earth's ocean tides (Dooley, 1995), with tidal generating forces varying inversely with the distance between masses. It is important to note the physical location of a tide on the earth's surface when studying tides because the angle between the earth's axis and the moon's orbit, known as the lunar declination, causes different points on the earth to experience diurnal, semi-diurnal, and mixed tides with a combination of either diurnal or semi-diurnal components. Diurnal tides are those that have one high and one low water a day (Dohler, 1996), as seen graphically in Figure 3.2 which represents a time period of one month. Semi-diurnal tides are those that have two high waters and two low waters daily (Dohler, 1996)(Figure 3.3). Mixed tides are a tide with two unequal high waters and two unequal low waters each day (Dohler, 1996), as seen in Figures 3.4 and 3.5 which represent the mixed, mainly diurnal and mixed, and mainly semi-diurnal patterns over a month.

The study area is a micro-tidal coast with a maximum tidal range of two meters and mixed tides that are mainly semi-diurnal. From Figure 3.6 it can be seen that the high water occurs almost simultaneously along all coastal points from Placentia Bay, Nfld, to Shelburne, N.S. The tidal range is not very great, with the difference between high and low water seldom exceeding two meters (Dohler, 1996).

3.2.2 Mechanical Effects on the Sea floor

The most common type of transient loading in the marine environment is that imposed at the sea floor by ocean tides. Sea floor formations are seen as behaving as porous

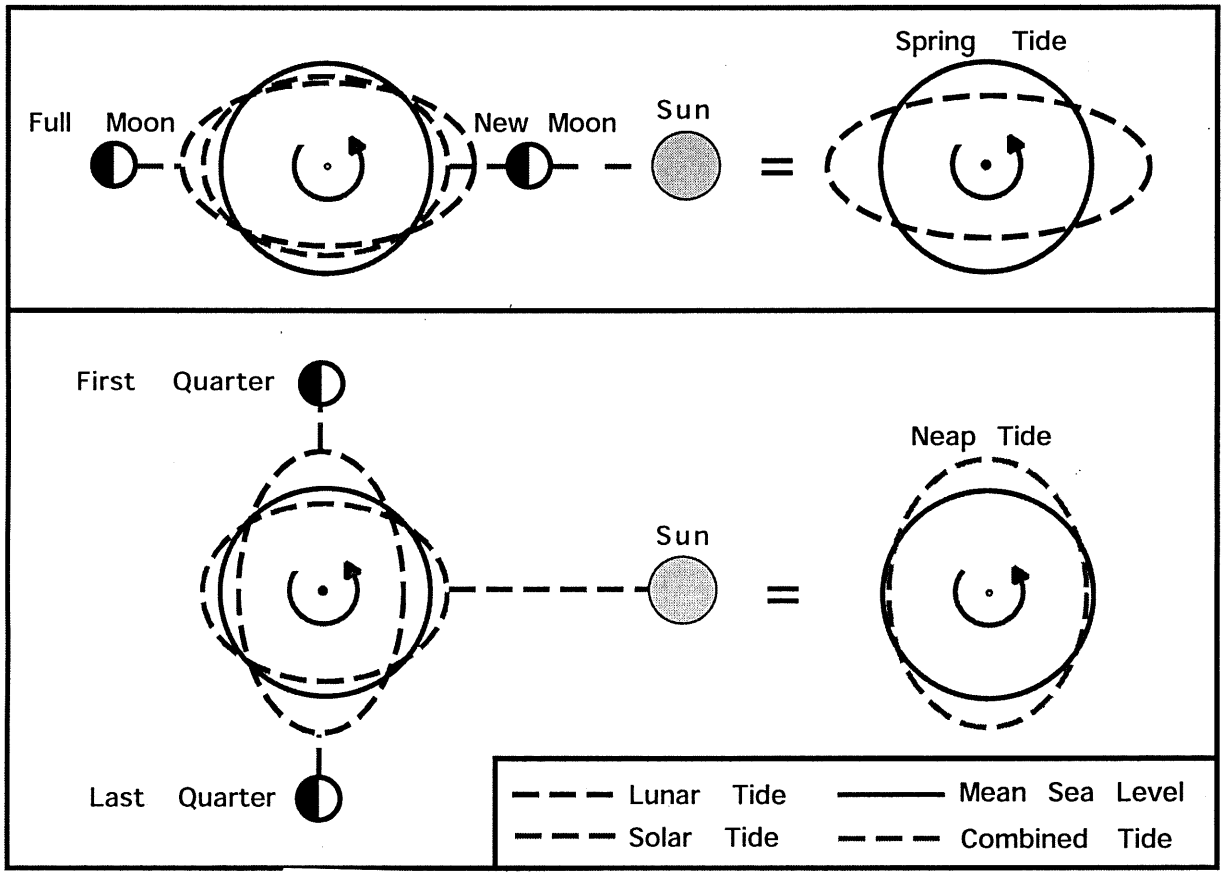

Figure 3.1 Gravitational Attraction.

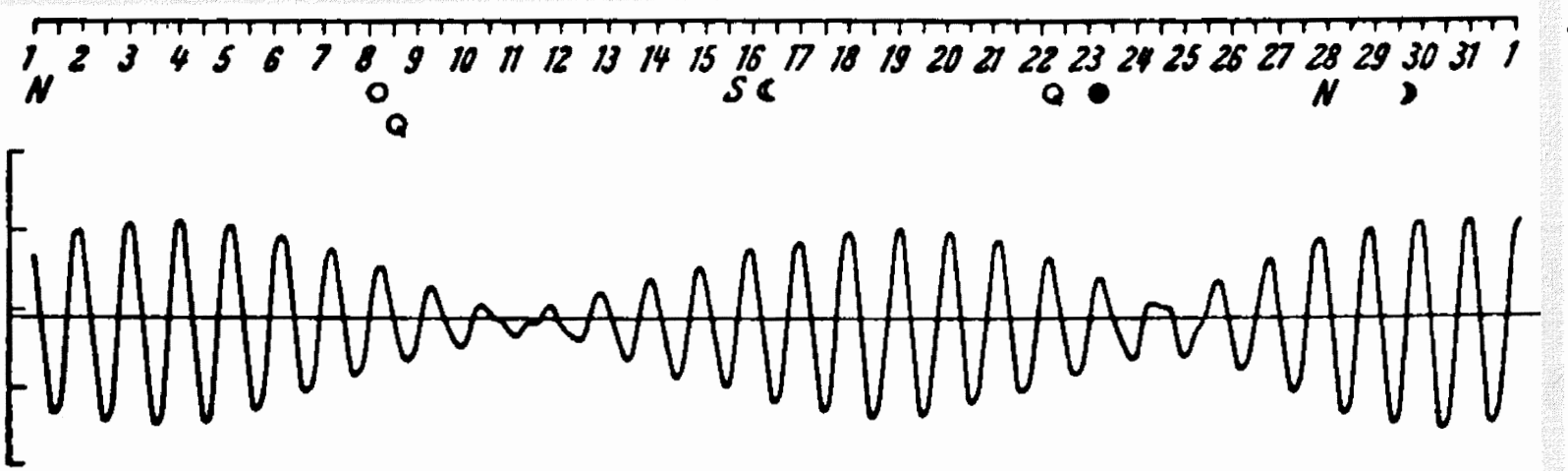

Diurnal: one high and one low water a day.

Figure 3.2 Diurnal tides (Dohler, 1996).

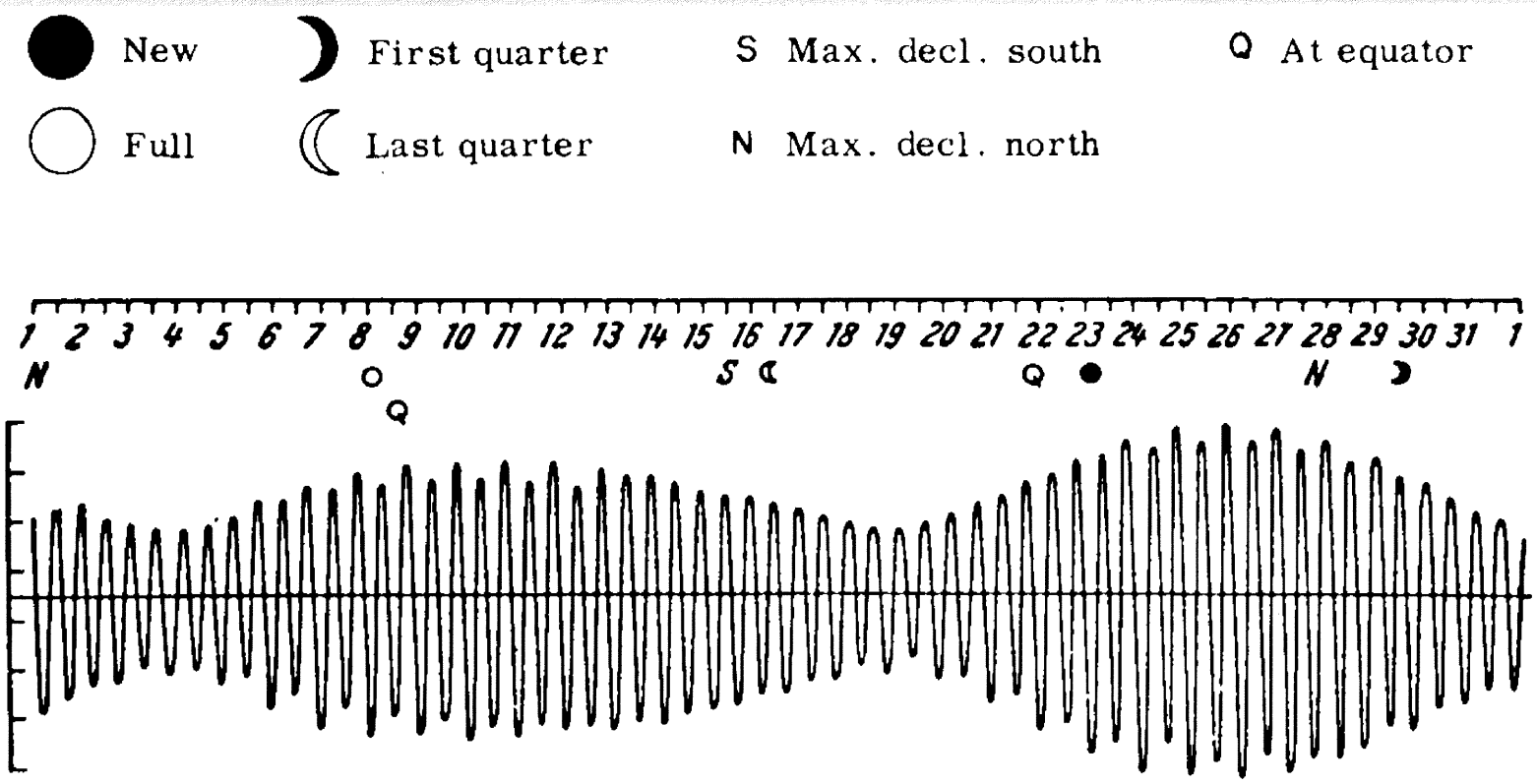

Semi-duirnal: two high waters and two low waters daily of approximately the same height; the interval between the transit of the moon and the occurrence of high water is nearly constant.

Figure 3.3 Semi-Diurnal tides (Dohler, 1996).

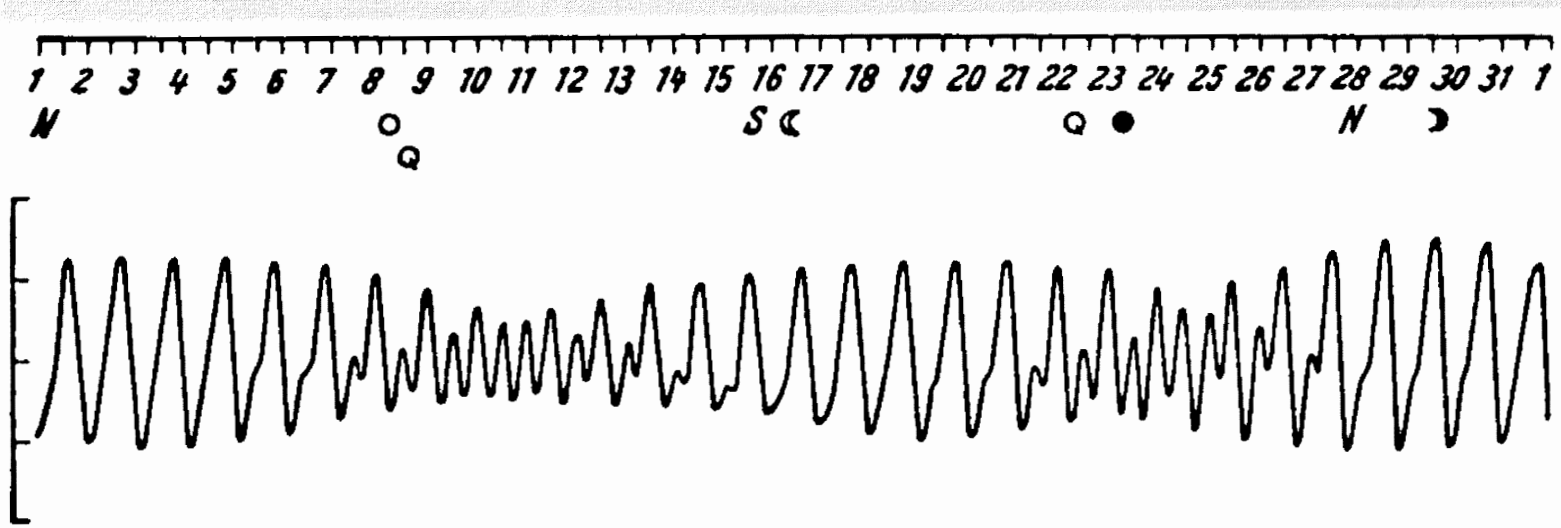

Mixed, mainly diurnal: occasionally there is only one high and one low water a day, following the maximum declination of the moon; at other times there are two large inequalities in height and time, especially when the moon has passed over the equator.

Figure 3.4 Mixed, mainly diurnal tides (Dohler, 1996).

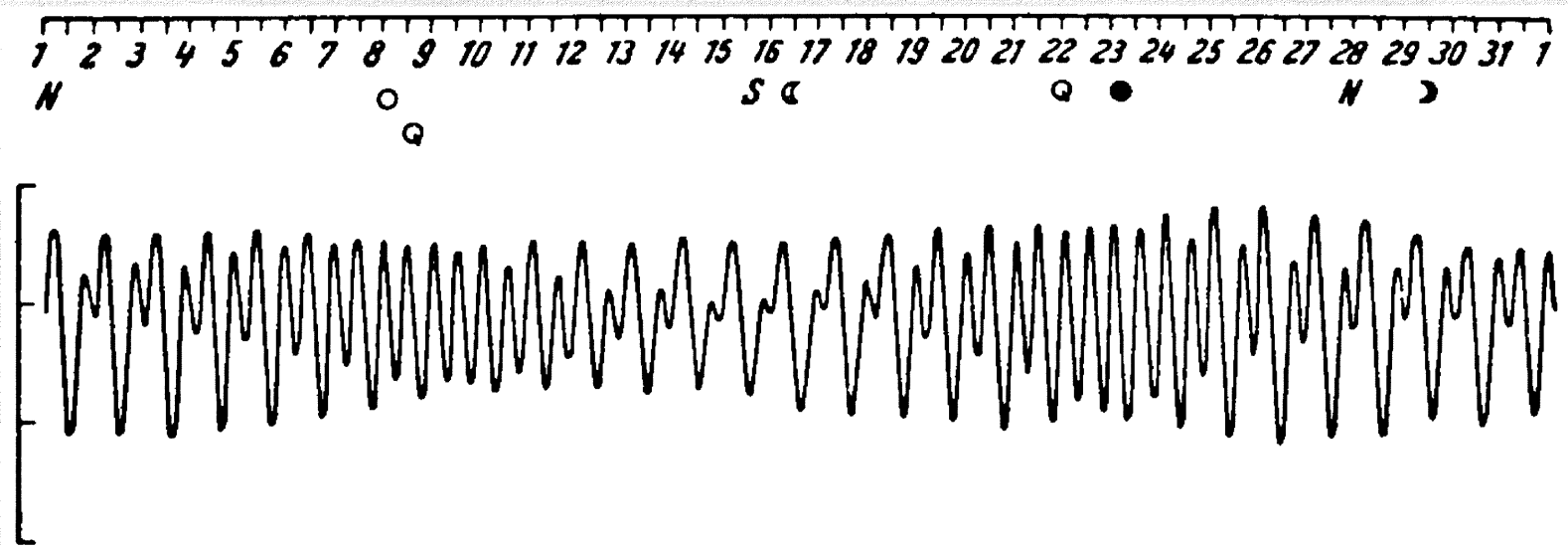

Mixed, mainly semi-dirurnal: two high waters and two low waters with inequalities in height and time reaching the greatest values when the declination of the moon has passed its maximum.

Figure 3.5 Mixed, mainly semi-diurnal tides (Dohler, 1996).

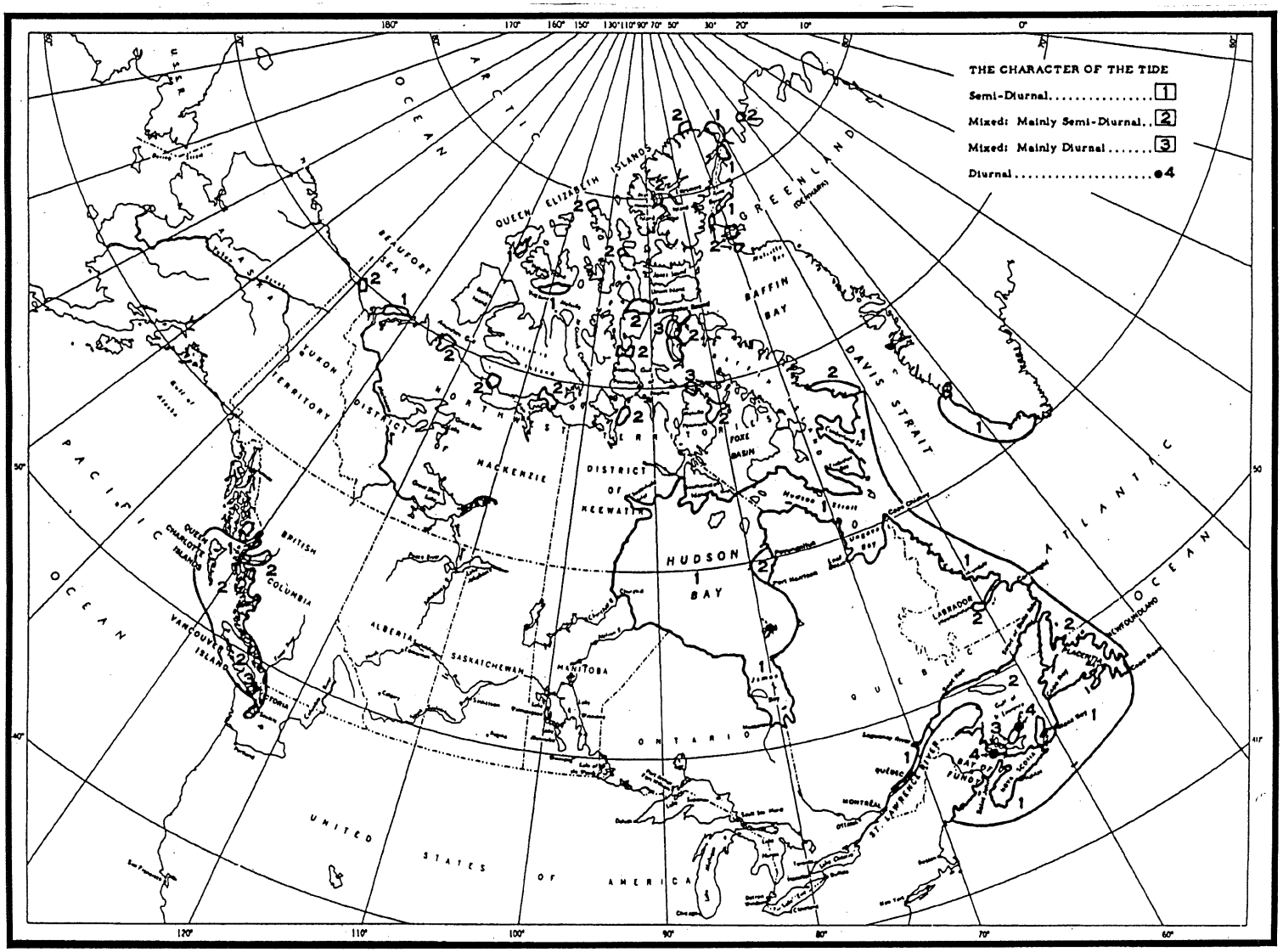
THE CHARACTER OF THE TIDE
Semi-Diurnal..... 1
Mixed: Mainly Semi-Diurnal.. 2
Mixed: Mainly Diurnal..... 3
Diurnal.....●4
ARCTIC OCEAN
GREENLAND
BAFFIN BAY
DAVIS STRAIT
BEAUFORT SEA
ALASKA
YUKON TERRITORY
DISTRICT OF MACKENZIE
DISTRICT OF KEEWATIN
HUDSON BAY
PACIFIC OCEAN
ATLANTIC OCEAN
BRITISH COLUMBIA
QUEEN CHARLOTTE ISLANDS
VANCOUVER ISLAND
ALBERTA
SASKATCHEWAN
MANITOBA
ONTARIO
QUEBEC
LABRADOR
NEWFOUNDLAND
UNITED STATES OF AMERICA
180°
170°
160°
150°
130°
110°
90°
70°
50°
30°
20°
10°
0°
120°
110°
100°
90°
80°
70°
60°
50°
40°

Figure 3.6

elastic media with respect to the influence of tidal frequency (Wang and Davis, 1996). A porous elastic medium is described by Wang and Davis (1996) as an elastic matrix framework of compressible grains hosting a compressible pore fluid. In many low permeability seafloor formations, tidal loading results in increased formation pore pressures that are driven diffusively. In the study area, the tidal loading results in advection, or fluid flow.

When dealing with tidally induced pressure variations in sea floor formations, current analysis and measuring techniques allow properties such as framework compressibility, permeability and gas content to be calculated within the formation (Van der Kamp, 1983). Among the properties involved, permeability, frame bulk modulus, and pore fluid bulk modulus are most likely to have the largest variability (Wang and Davis, 1996). In the marine environment an effective overburden pressure is placed on sediments at a certain depth (MacKillop, 1994); this is the buoyant weight of the overlying sediment.

3.2.3 Darcy's Law

Most groundwater flow that takes place can be described by Darcy's equation. According to Chapman (1981), Darcy's law, in practice, is a statistical relationship in which inhomogeneities are averaged out between manometer readings. Darcy's law is

$$Q = -KA\ (dh/dl) \qquad (3.1)$$

where Q is the flow rate, K is the hydraulic conductivity, A the cross sectional area, and dh/dl is the hydraulic gradient where h represents the height of measurement and l is the length of the measurement. Note that the hydraulic gradient, represents the change in

elevation over the length of a sample, is a dimensionless unit.

Hydraulic conductivity is the property of a sample which describes the rate at which fluid flows through it. Also known as Darcy's coefficient of permeability, hydraulic conductivity is commonly referred to as permeability (Holtz and Kovacs, 1981). The property of the sediment alone is known as the intrinsic permeability. The relationship between the hydraulic conductivity of a material and the intrinsic permeability of that material is expressed in the following equation:

$$K = k\rho g / \mu \qquad (3.2)$$

where K is the hydraulic conductivity, k is the intrinsic permeability, ρ is the density of the fluid, g is the gravitational acceleration, and μ is the viscosity of the fluid.

Looking at a simplified approach to Darcy's law would be to observe the characteristics across two layers. The two layers together behave as if they are one layer with respect to permeability and hydraulic gradient when measuring total flow within the layers. This kind of relationship when broken down to individual layers shows that there is inverse ratio between the two. This relationship can be expressed as

$$k_1/k_2 = \Delta\, h_2/l_2 \;/\; \Delta h_1/l_1 \qquad (3.3)$$

where the permeability (k_1, k_2) of the first layer would be half that of the second layer and the hydraulic gradient ($\Delta\, h_2/l_2$, $\Delta h_1/l_1$) of the second would be half that of the first layer. This application is very simple and in reality sediments vary in grain size, have variable sorting and have porosities that all may change along the flow path (Chapman, 1981).

Using an analytical expression of Darcy's law the follwing equation can be applied

$$Q = K\, i = K\, \Delta h/l \qquad (3.4)$$

where K the hydraulic conductivity and i equals the (Δh) loss of signal pressure over depth(l).

3.3 Water Level Data

3.3.1 Lingan Collieries

The mine workings of the Lingan Colliery now form part of the large 1B hydraulic system as described in Chapter 1. A vibrating wire monitoring system was setup by the CBDC to monitor this rising *in situ* water and provide hourly water level data.

3.3.1.1 Vibrating Wire Piezometers

The vibrating wire system uses either the AVW1 or the AVW4, with Geokon model 4500 vibrating wire piezometers and pressure transducers. A typical setup used by the CBDC for these monitoring stations is shown in Figure 3.7. The AVW1 and AVW4 systems are designed to operate over a temperature range of -25^{0}C to +50^{0}C. The sensor in the vibrating wire system uses a change in the frequency of a vibrating wire to sense water pressure and therefore, water depth for a sensor at a fixed depth (Figure 3.8). An increase in pressure presses the diaphragm upwards and thereby reduces the tension in the wire. In turn, the resonant frequency of the vibrating wire decreases. This change in frequency excites the plucking and pickup coils which create a "swept" frequency, which

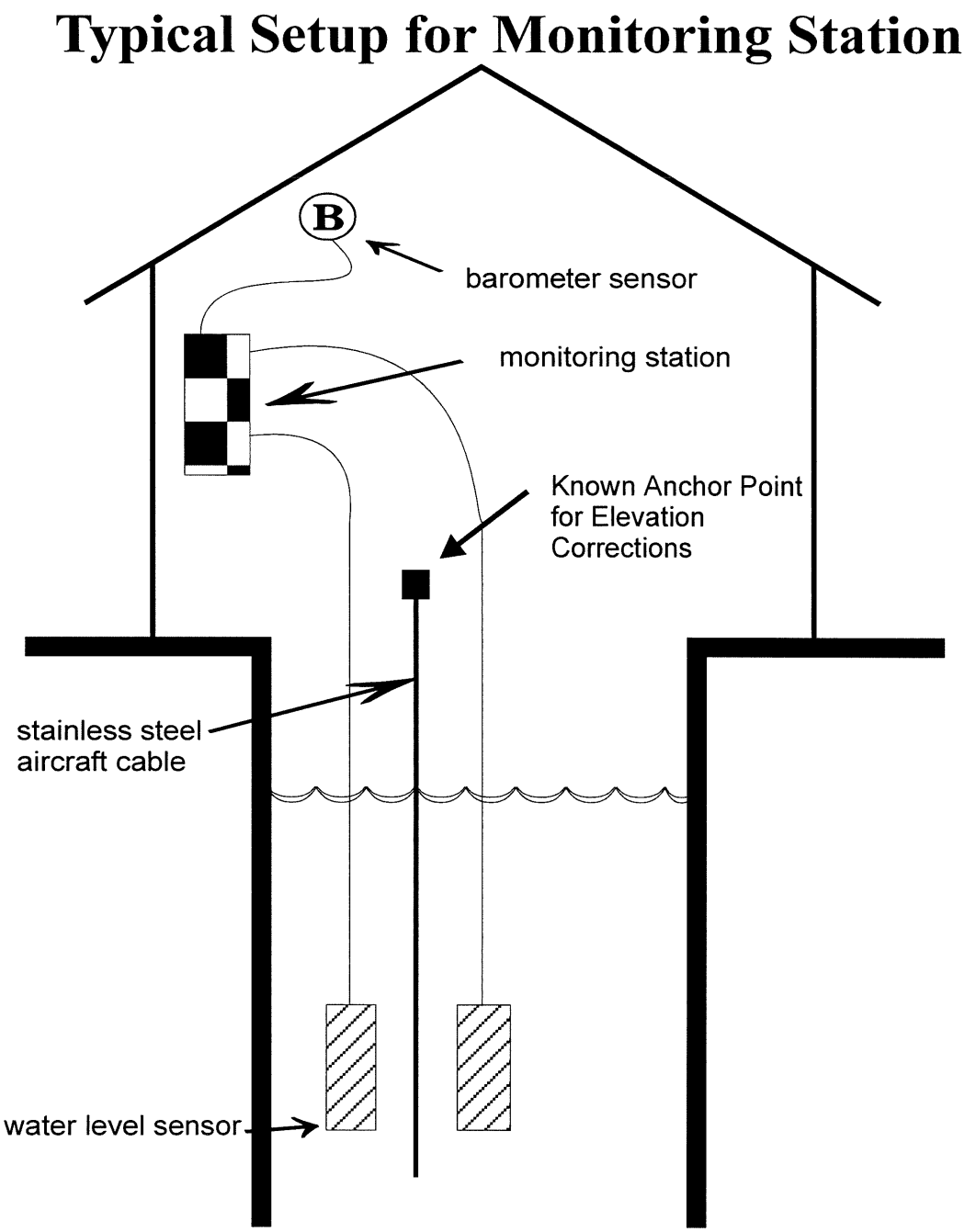

Figure 3.7 Showing the general setup for a monitoring station as used by the CBDC.

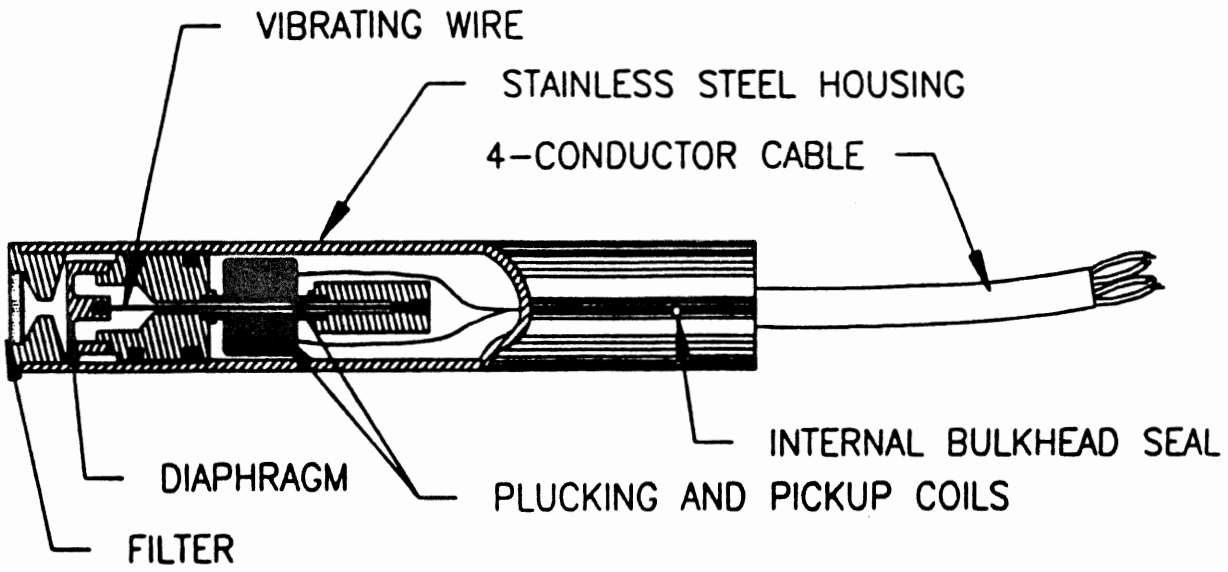

Figure 3.8 Vibrating Wire Diagram

is a group of different frequencies that are sent one after another. This "swept" frequency causes the wire to vibrate at each of the individual frequencies. The wire will vibrate with a resonate frequency for a period of time so that it cuts the lines of flux in the plucking and pickup coils, which will induce the same frequency on the lines to the CR10 datalogger and controller module. The CR10 will wait 20 milliseconds for non- resonant frequencies to die out and then it accurately records how much time it takes to receive a user defined number of cycles. From this data, the datalogger program converts pressure (psi) to an elevation or depth measurement. Actual setups that are used by the CBDC are seen in Figure 3.9.

3.3.1.2 Method of Correlation

The amplitude of the transmitted tidal waves decrease as the distance from the seafloor increases and the phase or time lag, of a maximum or minimum increases as the distance from the seafloor increases. This is illustrated by data for a time interval from November 7, 1994 to January 18, 1995. Figure 3.10 shows several frequencies, both low and high, that have overprinted the baseline rising water level record. To remove the trends and some outliers from these data, the data were de-trended and several manipulations were carried out. The first step in the de-trending process is to ensure that the units of measurement are the same, or at least the same system. Figure 3.11 shows the time period from November 7 and December 7, 1994 and the units of depth have been converted from feet (Figure 3.10) to centimeters to make later calculations less

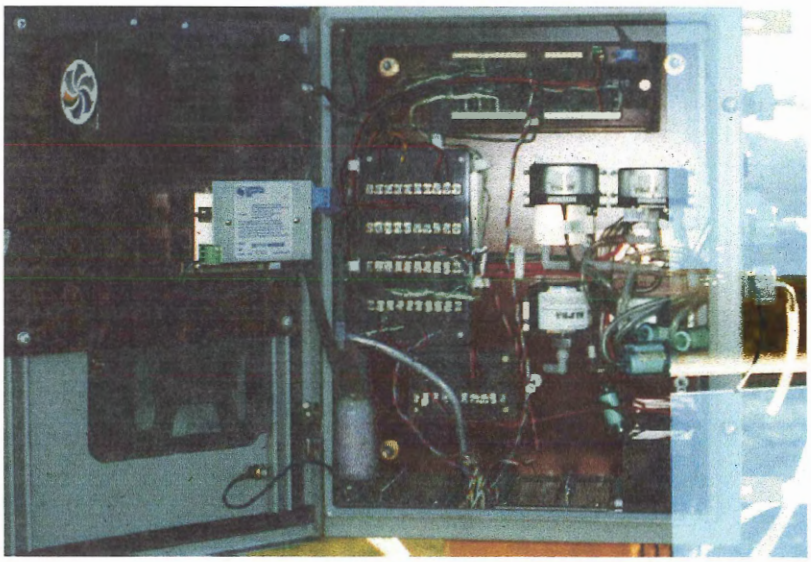

Photo A

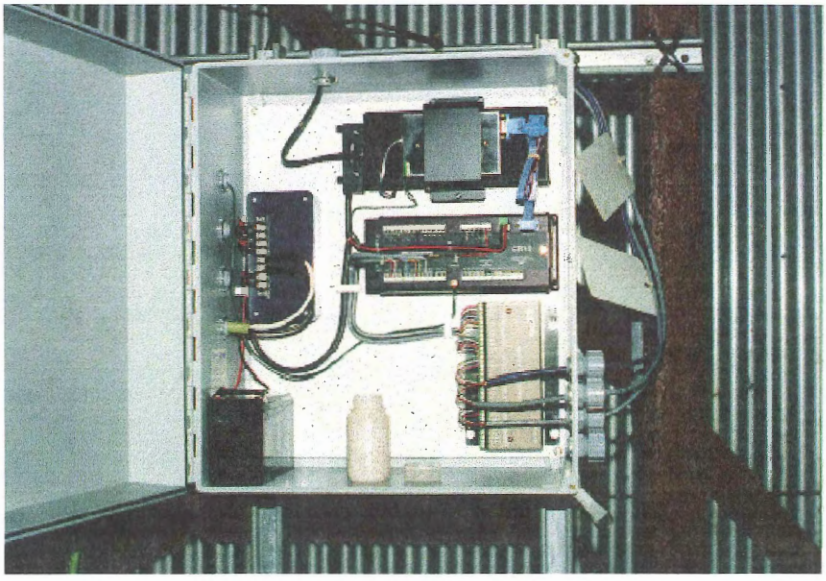

Photo B

Figure 3.9. Typical setups for mine monitoring stations. Photo A the gaseous void volume monitoring station at the No.12 Colliery vent stacks. Photo B is the water level station at Quarry Point for No.4 Colliery (Gary Ellerbrok, pers. comm., 1997).

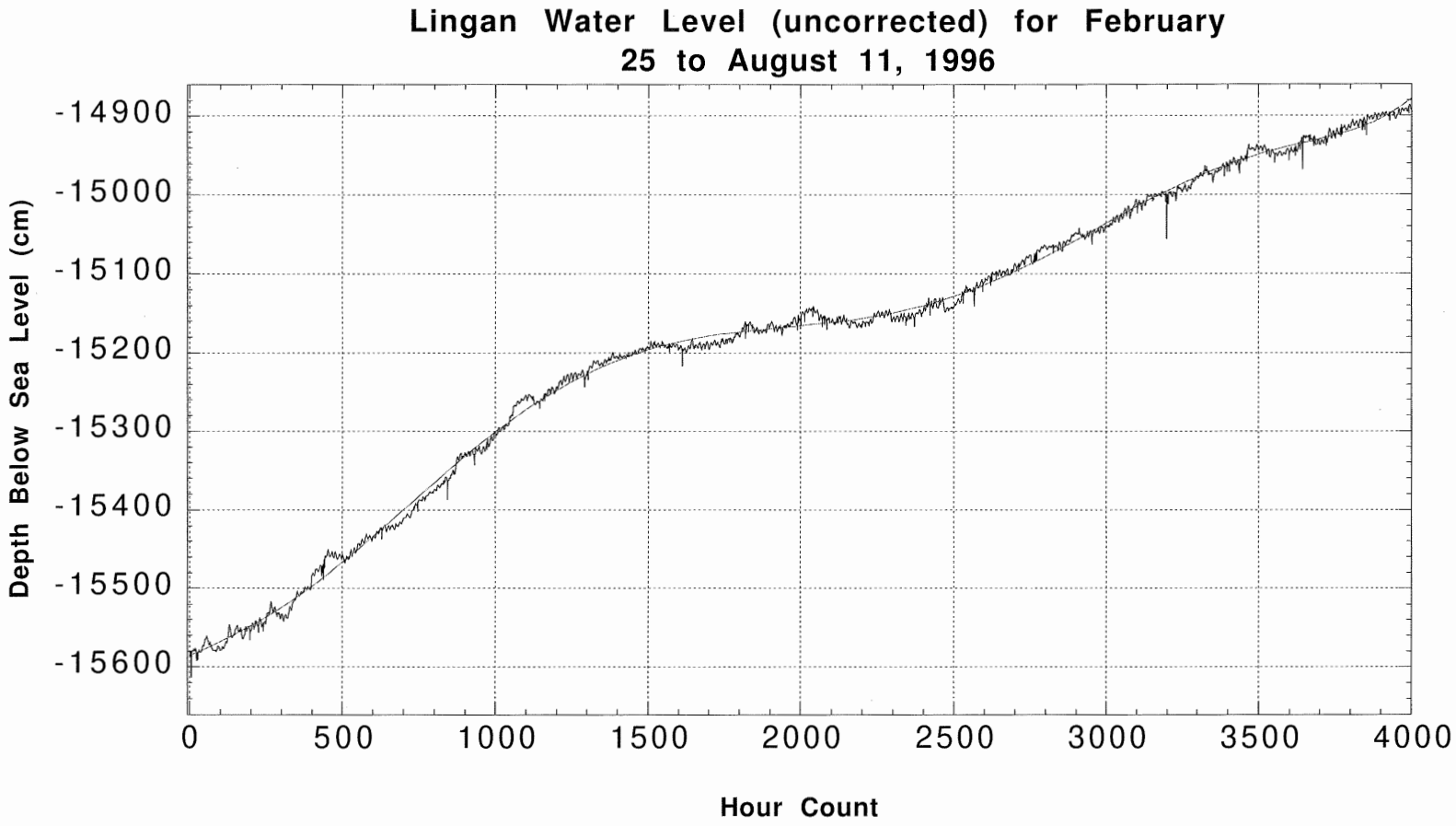

Figure 3.10 Lingan water level data for February 25 to August 11, 1996 which has not been de-trended. Several frequencies can be observed overprinting the baseline water level record.

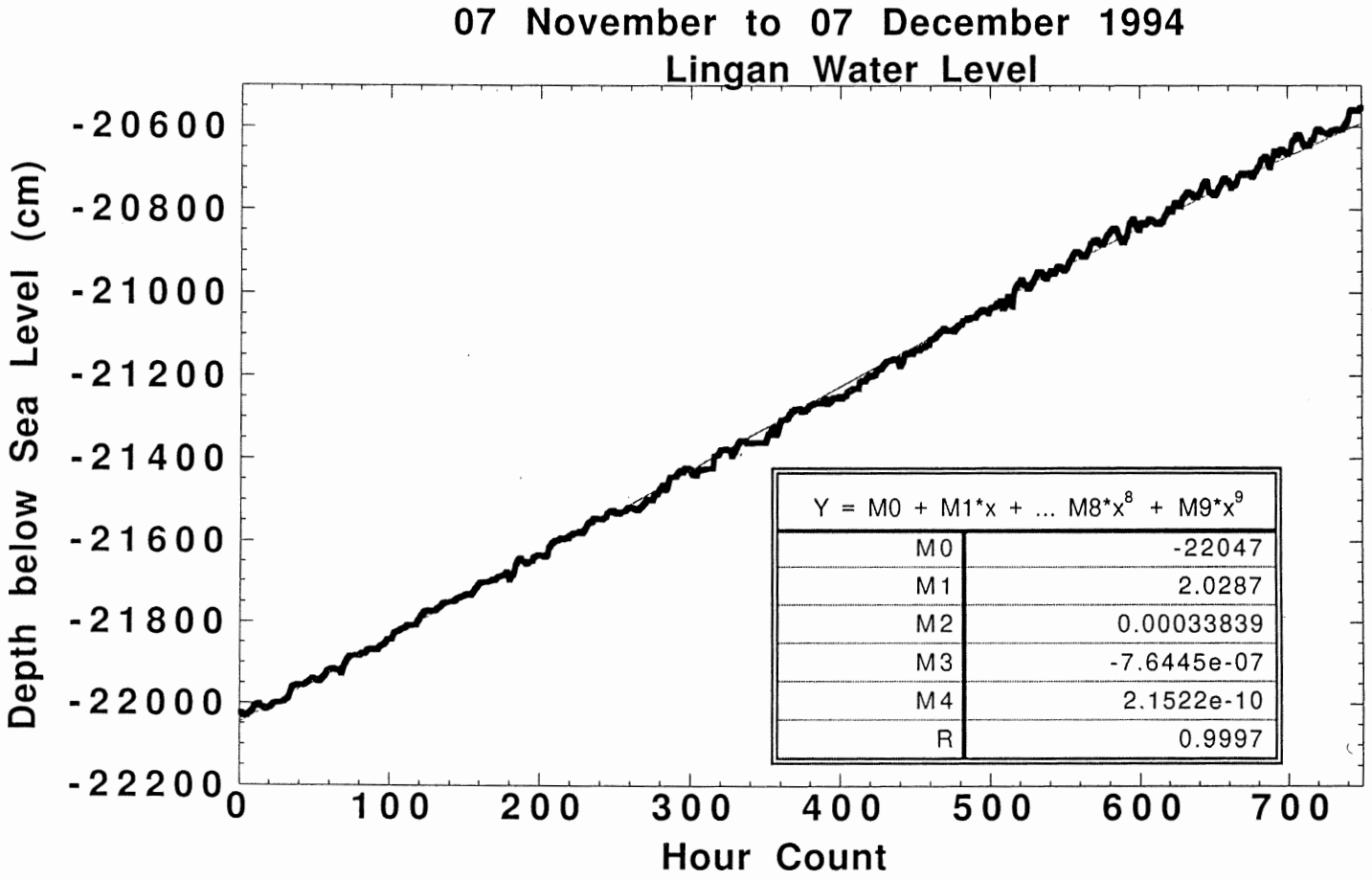

Figure 3.11 Lingan Water Level Data for November 1994.

involved. Calculating the best fit line for this slope is the next step, once the line of best fit is found it is used to move the slope of the best fit line to a slope of zero by simply using the lowest value as the base level. Then every value from the line of best fit has the base value subtracted away from it (Figure 3.12). The slope of zero improves correlation between the frequency of the mine water level data and the tidal data frequency because they both are plotted with the same relative scale. Figure 3.13 shows a record that represents the type of tidal signals that are present in the study area. The correlation of the phase and amplitude shifts between the two sets of signals are discussed in Chapter 4.

3.3.2 Sydney Basin Tidal Data

In Sydney Harbour, Environment Canada's tidal station number 612 records daily oceanographic data such as ocean tides, water and air temperature, barometric pressure and the velocity and direction of ocean currents (Dohler, 1996). The information collected from this station includes hourly tidal water elevation records. This information is recorded and quality assurance carried out by Environment Canada before it is released to the public. The standards set by Environment Canada, and enforced during the data collection provides this study with a means of control on signal quality. The signal 'purity' provides us with a time constant with which to compare the mine water level data.

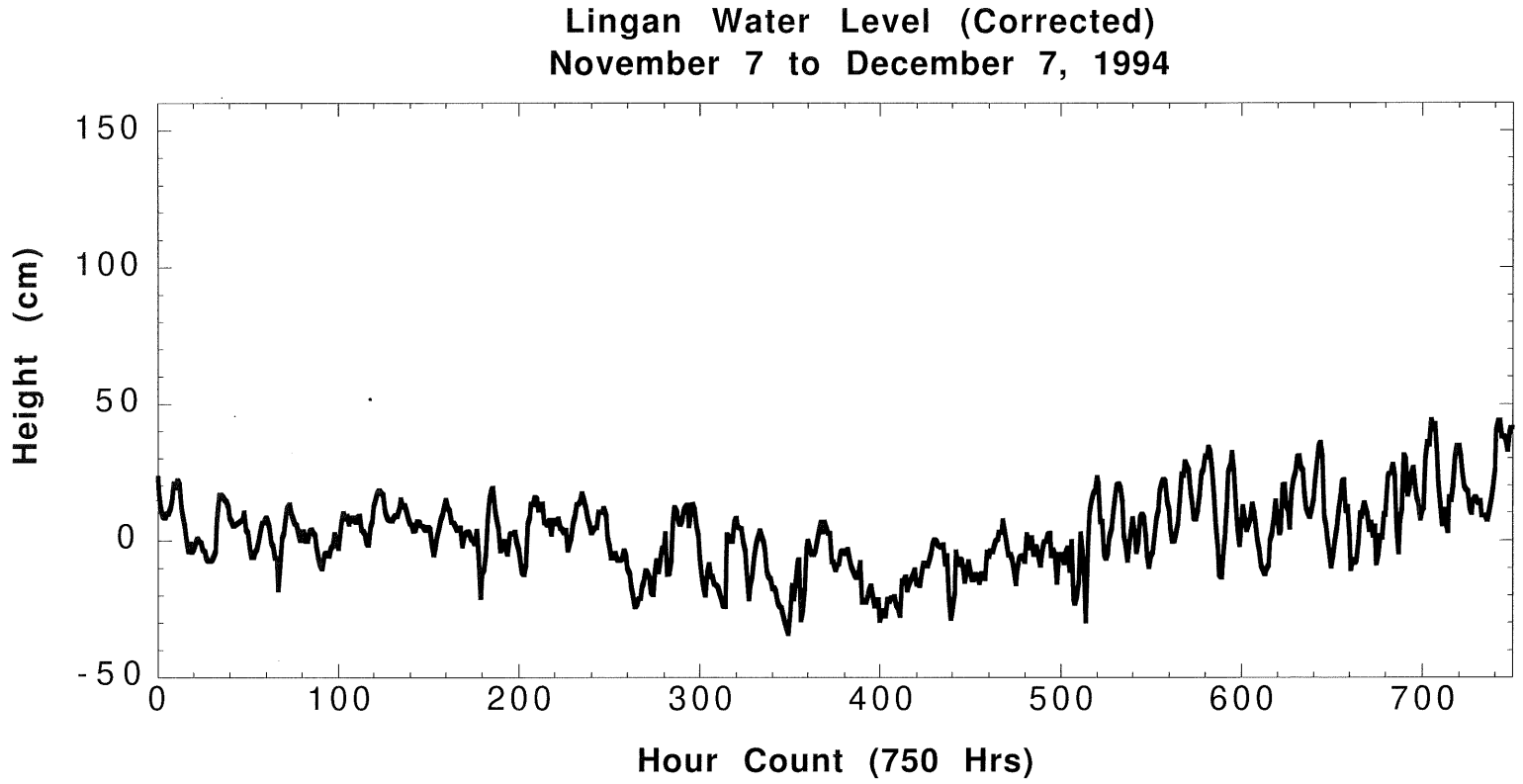

Figure 3.12 Lingan water level for November 1994 that has been detrended.

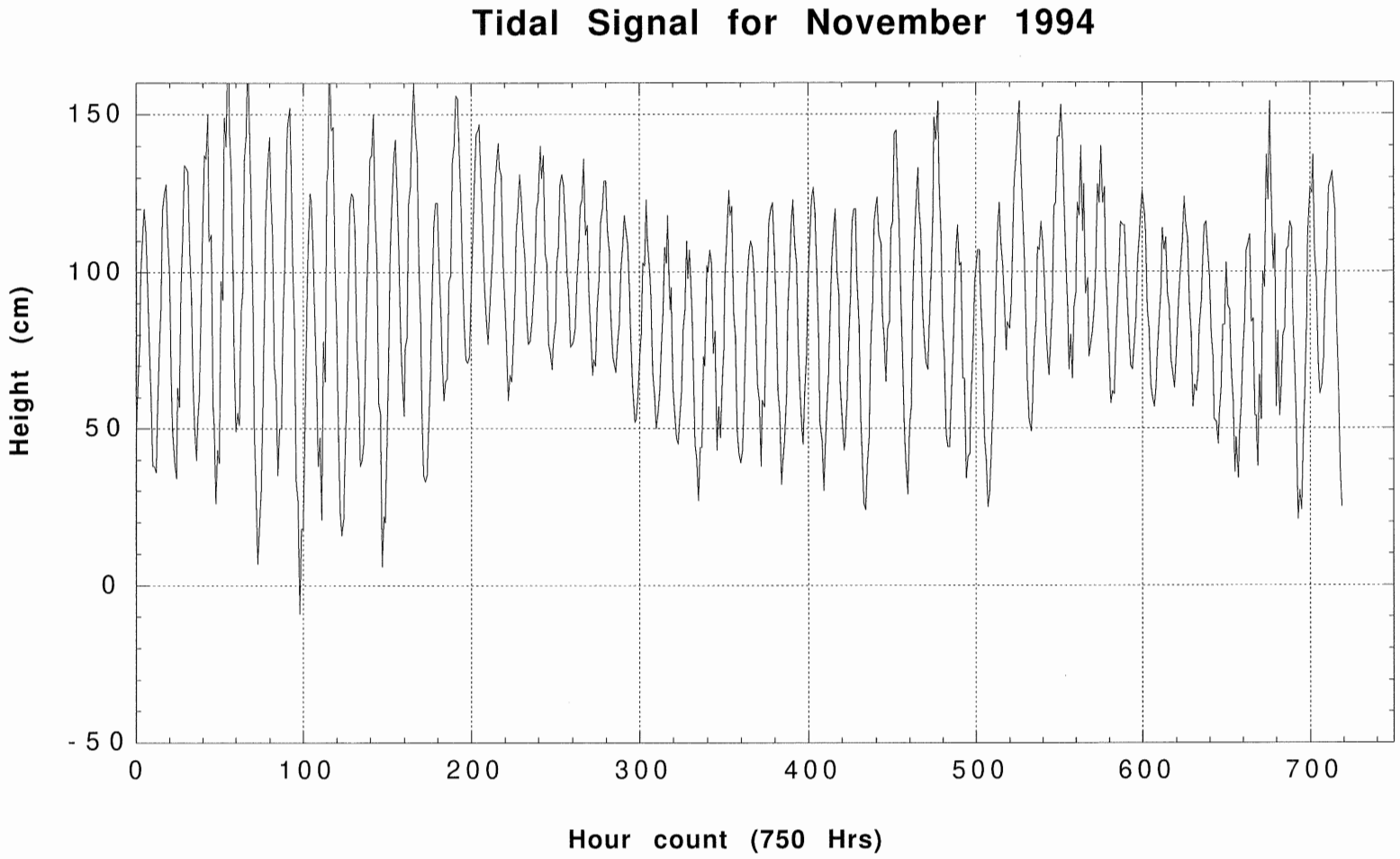

Figure 3.13 A typical tidal signal that is found in the study area off the coast of Cape Breton

CHAPTER 4 PERMEABILITY DATA

4.1 Introduction

The application of water level fluctuations for determining *in situ* permeability is made with the assumption that the Lingan mine is effectively separated from the ocean water by an extensive confining layer, which in the vertical is defined as the region between the sea floor and the Harbour seam. Fluctuations in mine water levels is assumed to be in response to the changing load on the confining layer from the tidal cycles (Ferris et al, 1962). As the tide rises, the load on the confining layer is increased, which causes an increase in water level within the mine. The reverse process occurs as the tide lowers (Ferris, 1963).

Using this approach the data is configured to try and match the two signals so that correlations in phase and amplitude shifts can be sought. Techniques for doing both of these are discussed in more detail in later sections of the chapter.

4.2 Processing Data

4.2.1 Tidal Data

Environment Canada corrects its data by performing quality assurance on all the data points retrieved from their tidal stations. This quality control ensures that the tidal data is accurate and consistent (Figure 4.1). As seen from the tidal frequency data, there are distinctive signatures to most peaks in these mixed, mainly semi-diurnal tides.

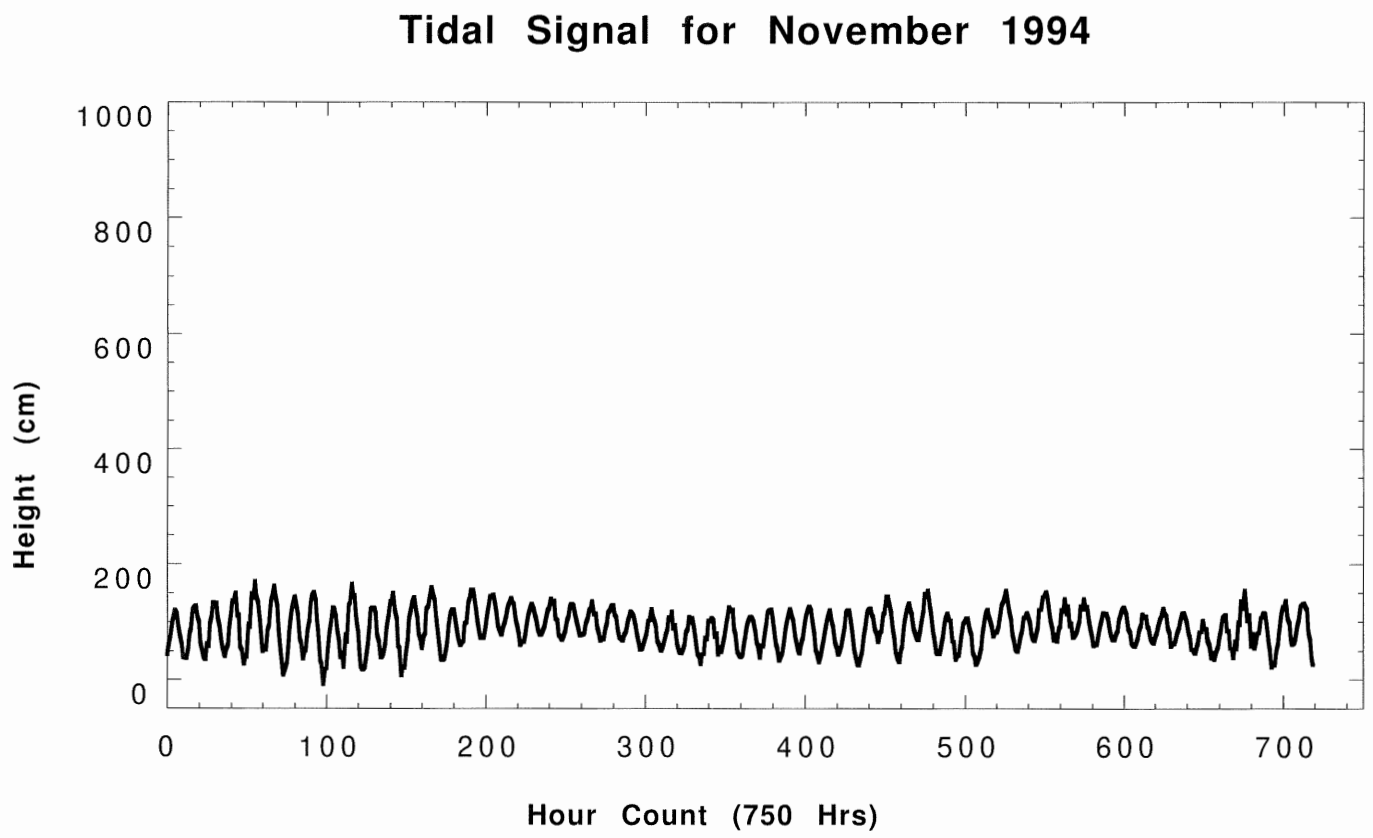

Figure 4.1 Tidal signal for November 1994 where the distincitive signal can be seen.

4.2.2 Lingan Water Level Data

The water level data from the Lingan mine show that there are clearly influences on these records that are causing them to change their physical appearance while the water levels are rising (Figure 4.2). The signals need to be de-trended so that they can be observed without overprinting by the increasing water level signal. This is achieved by taking the slope of the best fit line and moving it so that it has a slope of zero, as described in Chapter 3 (Figure 4.3). For consistency the mine water level data were all converted to metric units, specifically, centimeters below sea level.

Once the mine water level data has been de-trended and placed on the correct scale, the next step is to observe the data graphically and look for sections that may be influenced by external influences such as precipitation run-off into the mine, movement of large amounts of equipment into or out of the Phalen workings, and mining operations such as blasting. Another factor that needs to be considered for both the mine water level data and the tidal data are recording errors that occur due to electronic constraints. The equipment needs to be tested and calibrated at regular intervals to maintain a consistent level of data quality.

These types of influences, either physical or electronic, can cause the reading to be erroneous by giving a false water level. Figure 4.2 shows a time period where the data was influenced for one reason or another with the end result of a false section within the water level data. These sections must be avoided in the analyses because they do not represent only the transmitted tidal signal. For this reason, some monthly intervals in the overall two year period of the study have not been considered in the analyses.

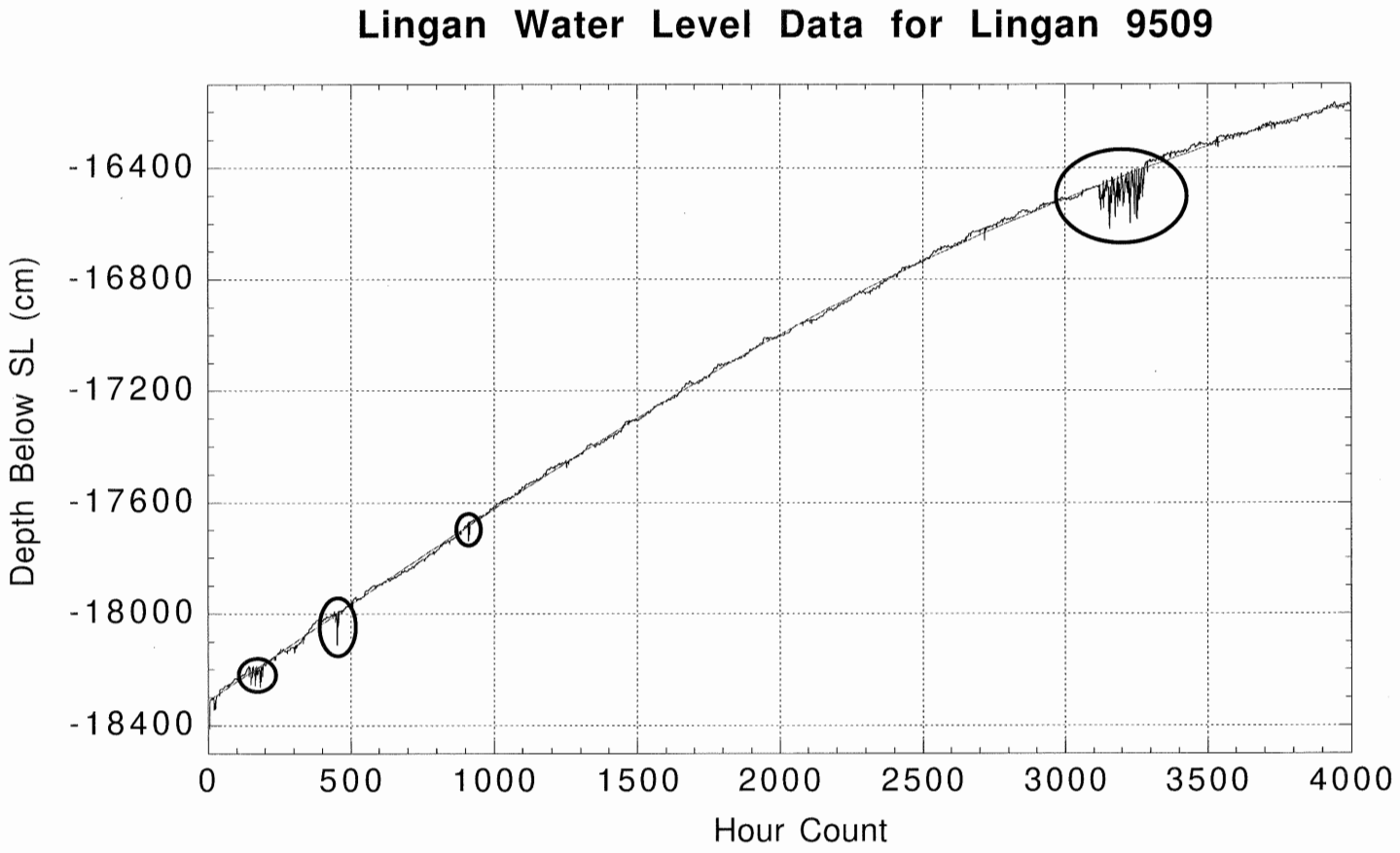

Figure 4.2 Lingan water level data showing contaminated or corrupted sections. Sections are shown in the circled regions.

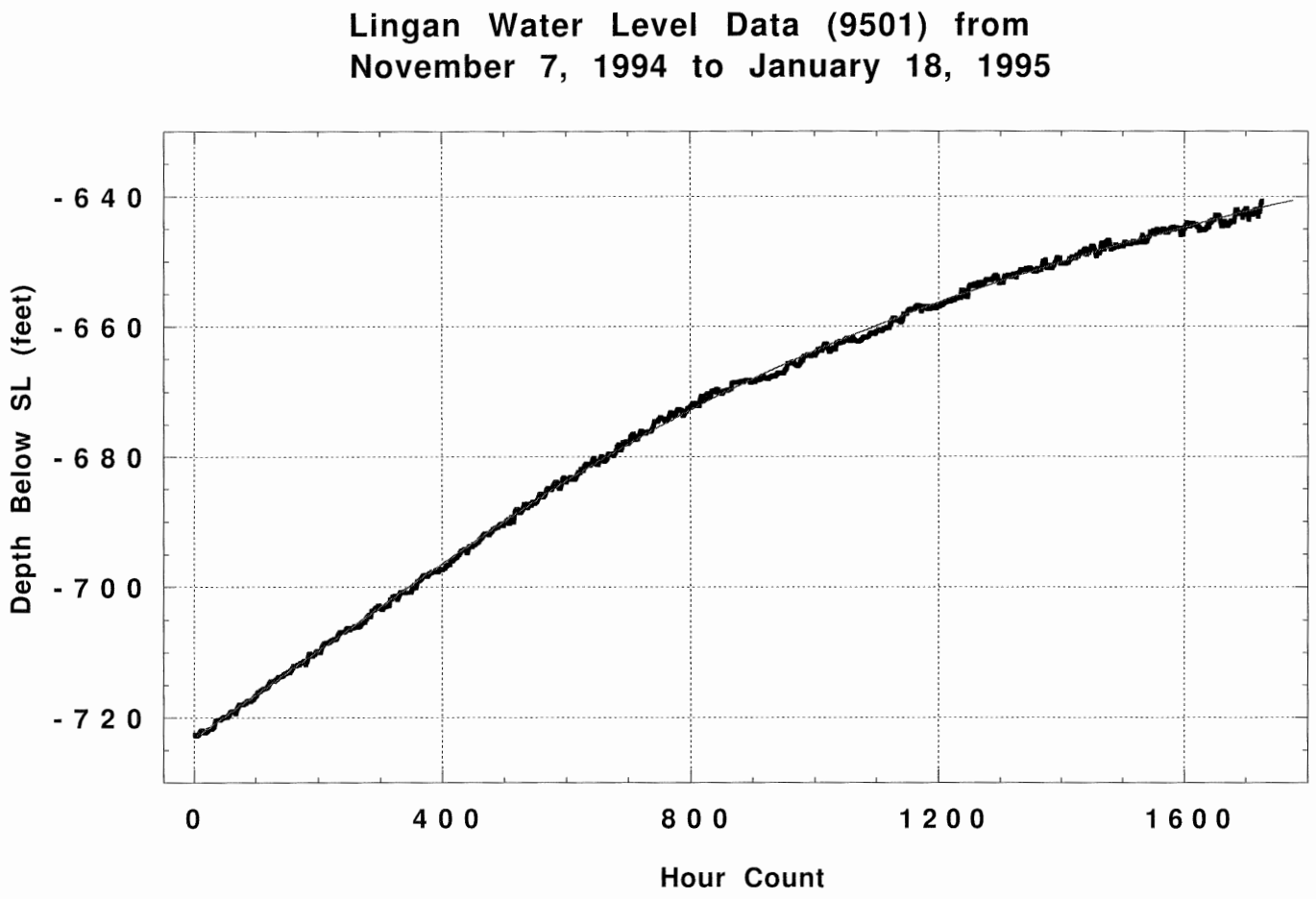

Figure 4.2a . Lingan Water Level uncorrected for the period spanning November 7, 1994 to January 18, 1995.

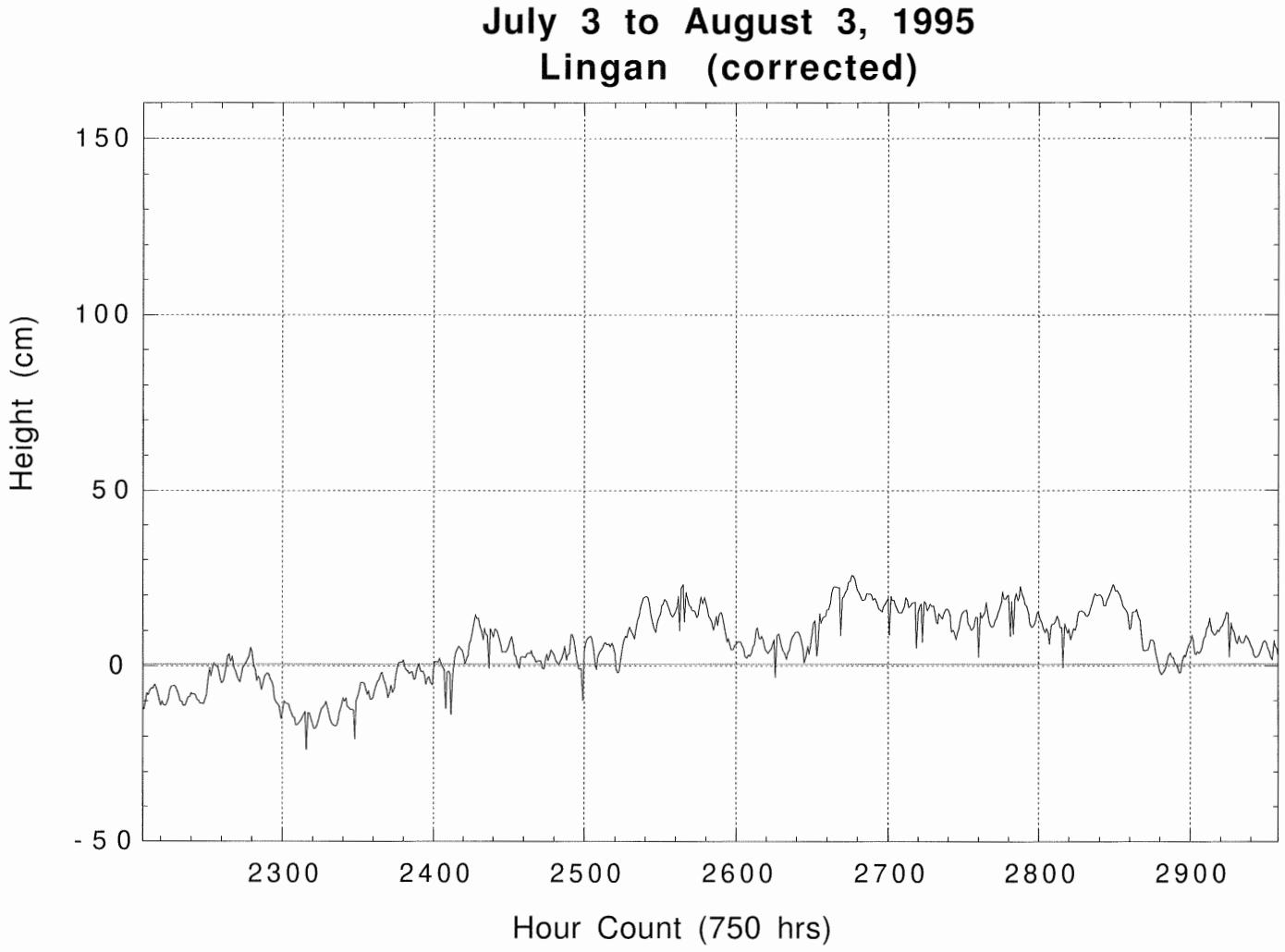

Figure 4.3 De-trended Lingan water level for July1995

4.3 Correlating Data

4.3.1 Phase Shift

The phase shift is used to calculate the difference in arrival times of the peaks and troughs of the tidal signal, between the mine and ocean tidal signals. This flow provides us with a unit of measurement in hours that is converted to seconds to calculate a flow velocity with the known depth to water level in the mine from sea level. This velocity, together with the amplitude shift, is used to calculate the hydraulic conductivity (permeability) of the section.

Examples of phase shift measurements are seen in Figure 4.4 and Figure 4.5 with Figure 4.4 representing the tidal signal and Figure 4.5 representing the mine peak that corresponds to the tidal peak. It is the difference between the mine and tidal peaks that represents the phase shift. Phase shift observations for a period from November 1994 to Sept 1996 are seen in Appendix A.

4.3.2 Amplitude Shift

The amplitude shift is the difference between the peak heights under the tidal curves and the mine water level curves. Figure 4.4 and Figure 4.5 also show tidal and mine water level amplitude lines as well. The difference between these lines is the amplitude shift. The hydraulic gradient is calculated from the difference between these heights using:

$$i = dh/dl \qquad (4.1)$$

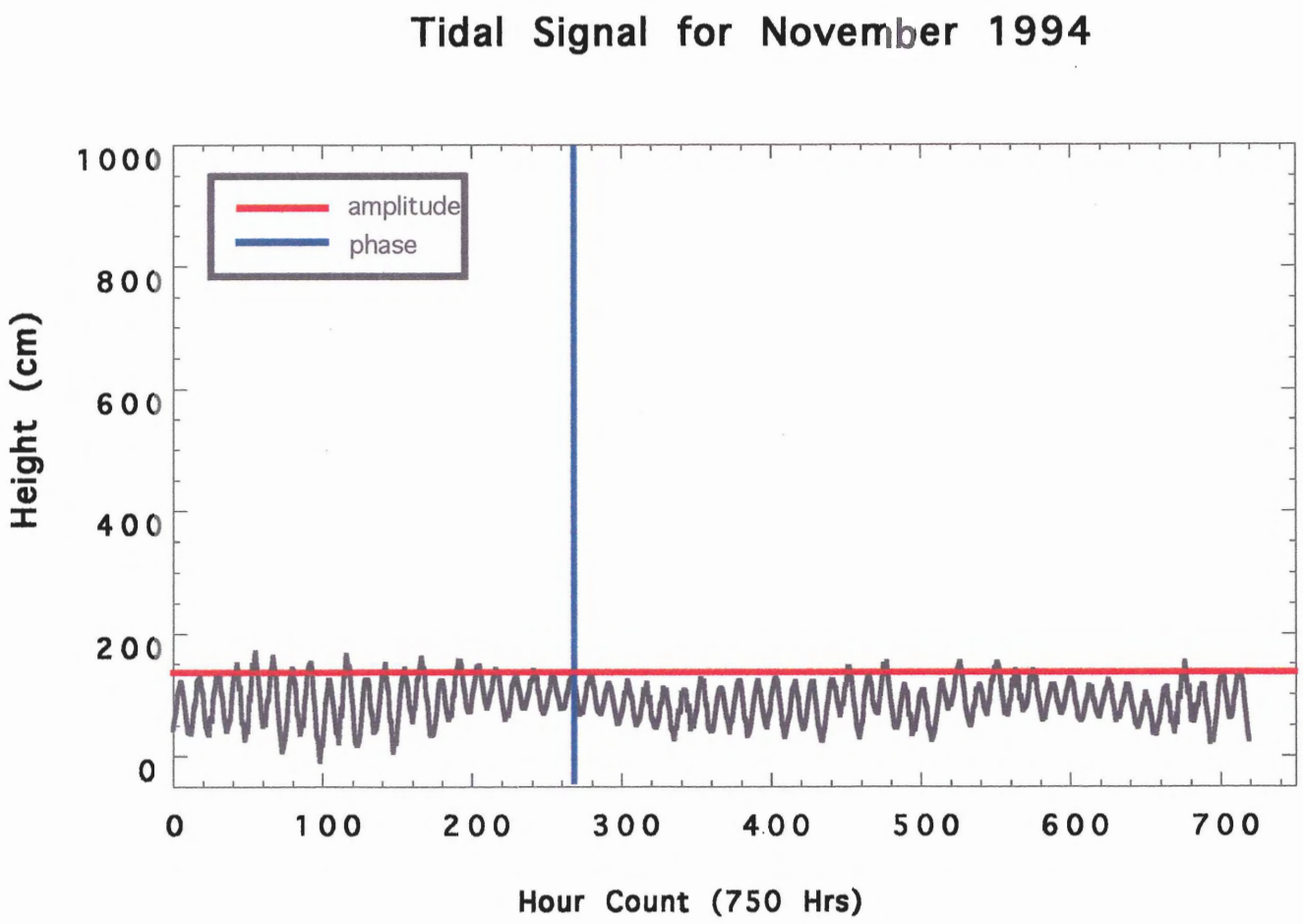

Figure 4.4 Tidal Signal for November 1994 with a peak matched to a peak in the Lingan mine water level data. Amplitude and phase measurements are represented by the red and blue lines.

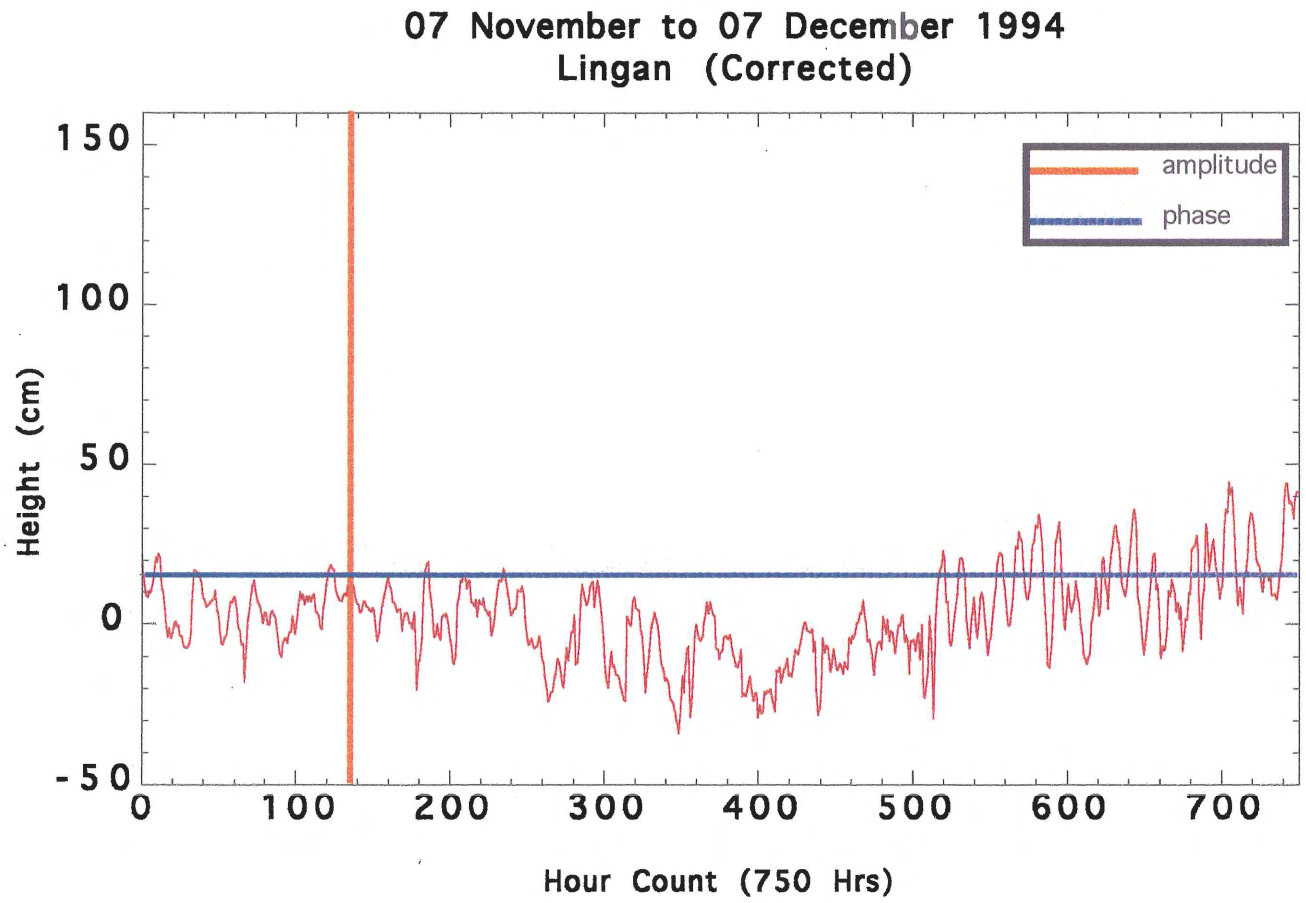

Figure 4.5 Graph of Lingan water level data (corrected) for November 1994.

4.4 Calculating Permeability

The permeability results come from the following relationship, which states that the apparent velocity (v) of the transmission of a wave is

$$v = x/t \qquad (4.2)$$

where x is the distance from the water level in the mine to sea level and t is the time difference between peaks, in this case it is the phase shift. This equation indicates the apparent velocity of a maximum or minimum and does not refer to the rate of pressure transmission (Ferris, 1963).

As seen from Appendix A, the ranges of phase shift are as low as 9 hours (32400 seconds) and as high as 14 hours (50400 seconds). The velocity (v) is used to calculate the hydraulic conductivity (k) using the principle of Darcy's law:

$$k = v/i \qquad (4.3)$$

where i represents the hydraulic gradient across the section between the Harbour seam and the seafloor, calculated from the difference in amplitude. Values for the amplitude shift are given in Appendix B.

The permeability results from the time period of November 1994 to September 1996 are given in Appendix C.

CHAPTER 5 DISCUSSIONS/RESULTS

5.1 Introduction

The hydraulic conductivity results in Appendix C represent the cumulative permeabilities that are found throughout the rock facies between the seafloor and the Harbour seam. The permeability of this zone is expected to be affected by previous and current mining operations. The type of mining methods used by the CBDC in Lingan included room and pillar and the longwall methods. Longwall mining encourages large scale stress redistribution by inducing the overburden to massively cave. (Reddish *et. al.*, 1994). The caving process that occurs above the longwall extraction involves fracturing and bed separation. These fractures and the bed separation cause permeability values to increase, in some cases by as much as two orders of magnitude (Whittaker *et. al.*, 1978).

At Lingan a single seam was mined, which affected the strata from the mine to the seabed. The resultant ground movement above the Phalen workings, however, will not only affect the seabed, but also the Lingan workings (Reddish *et. al.*, 1994). The subsidence associated with the longwall mining panels is the most important point of entry for groundwater infiltrating the workings. This occurs through drips and streamers in the roof of the mine workings (CBDC, 1994).

5.2 Permeability Prediction

The method used in this thesis provides the basis for some interesting evaluations of the present geological strata and the effects of the CBDC mines. The determination of

formation permeability, as determined by this project, is one of several aspects of rock characteristics that can be evaluated without actually sampling the rocks.

Before looking at permeability results, it can be predicted that the permeability of the region should fall in a relatively moderate permeability range. Permeability of rocks can vary by orders of magnitude, for example between shales and aquifer sandstones (Fetter, 1994). The results suggest that we are dealing with material that falls into the range of silts to sands as given in Table 5.1, which shows geologic materials and their usual ranges of hydraulic conductivities and permeabilities.

The results of this study show that the main permeability and rock material in the study area falls into a range between 1.77×10^{-3} to 9.20×10^{-2} cm/sec or 1840.8 to 95680 millidarcies (mD). The conversion to millidarcies from cm/sec is taken from Table 5.1, by multiplying the hydraulic conductivities by 1.04×10^{6}. This range of permeability is consistent with the lithologies present between the sea floor and the Harbour seam. A problem that arises from this result is that this implies that the high permeabilities are found in all directions. This does not appear to match the expected permeabilities when looking at bedding from the seafloor to the Harbour seam.

The vertical permeability of this section would be expected to be rather low due to the numbers of layers that exist and the intermixed, low permeability, mudstone and coal layers. One would expect to be dealing with a mainly heterogeneous anisotropic environment, where higher permeability would be found in the shallower sediments, parallel to bedding. The permeability data presented in Appendix C, however indicates

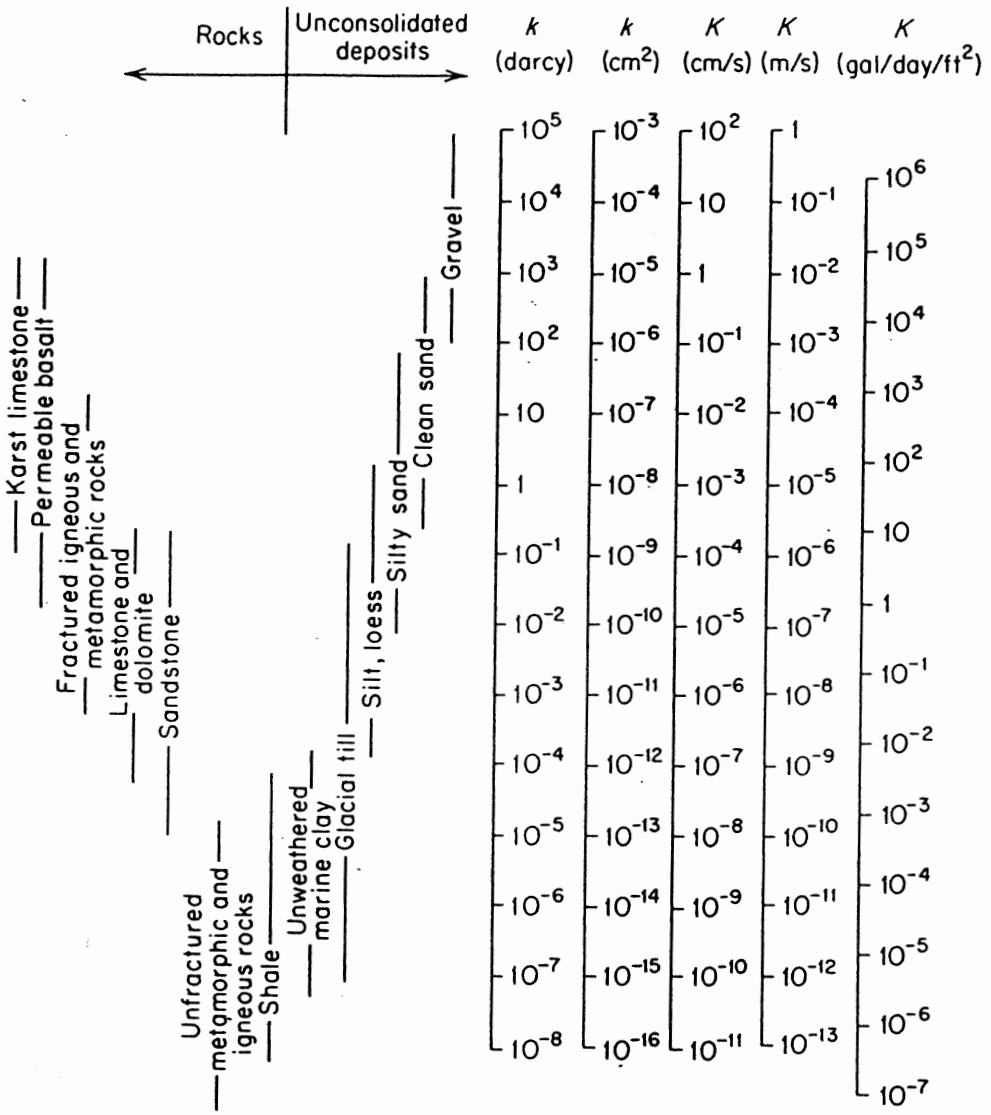

Table 2.3 Conversion Factors for Permeability and Hydraulic Conductivity Units

	Permeability, k*			Hydraulic conductivity, K		
	cm^2	ft^2	darcy	m/s	ft/s	U.S. gal/day/ft^2
cm^2	1	1.08×10^{-3}	1.01×10^{8}	9.80×10^{2}	3.22×10^{3}	1.85×10^{9}
ft^2	9.29×10^{2}	1	9.42×10^{10}	9.11×10^{5}	2.99×10^{6}	1.71×10^{12}
darcy	9.87×10^{-9}	1.06×10^{-11}	1	9.66×10^{-6}	3.17×10^{-5}	1.82×10^{1}
m/s	1.02×10^{-3}	1.10×10^{-6}	1.04×10^{5}	1	3.28	2.12×10^{6}
ft/s	3.11×10^{-4}	3.35×10^{-7}	3.15×10^{4}	3.05×10^{-1}	1	6.46×10^{5}
U.S. gal/day/ft^2	5.42×10^{-10}	5.83×10^{-13}	5.49×10^{-2}	4.72×10^{-7}	1.55×10^{-6}	1

*To obtain k in ft^2, multiply k in cm^2 by 1.08×10^{-3}.

Table 5.1 Range of Values of Hydraulic Conductivity and Permeability

that the situation could be more homogeneous than expected.

Another complicating factor is the removal of parts of the strata through mining, which affects the redistribution of stress within the sediments and the bedding planes. These stress changes are at their highest levels closest to the mine working. As the distance from the working increases the stress redistribution decreases. This redistribution of stress usually results in the fracturing of the medium in which it occurs (Whittaker *et. al.*, 1978). This fracturing results in an increase in the permeability of the media. Whittaker *et. al.* (1978) examined the effects of longwall mining on ground permeability. They concluded that the largest zone of change of *in situ* permeability lies between the face line and approximately forty meters above and forty meters behind the longwall face. The rocks studied by Whittaker *et. al.*, (1978) are similar to those found in our study area. There are multiple layers of sandstone, siltstone, shale, and coal which are very similar in thickness and structure to those found in the Sydney Mines Formation.

5.3 Hydrostratigraphic Units

The CBDC has recognized that there are two hydrostratigraphic units within the Morien Group, one being in the South Bar Formation the other being in the Sydney Mines Formation. The upper Morien hydrostratigraphic unit, found in the Sydney Mines Formation, contains both aquitards and aquifer complexes (CBDC, 1994). The aquifer complexes are composed of interbedded sandstones, siltstones, and shale facies. The combination of these facies in the aquifer complex tend to result in units of higher permeabilities than those found in the aquitards. These slightly more permeable units are

interlayered with the aquitards, which tend to be composed mainly of the coal seams and mudstone units, which have much lower permeabilities that the aquifer complexes. Values of the aquitard permeabilities generated from packer and slug tests, range from 1 x 10^{-5} to 1 x 10^{-7} cm/sec or 0.104 to 10.4 millidarcies (mD) (CBDC, 1994). The range of bulk permeability values for the aquifer complexes are between 1 x 10^{-3} and 1 x 10^{-5} mD. These ranges are lower than the 1840.8 to 95680 mD range that is calculated using the method defined by this project.

The application of Darcy's law to laminar flow over such a large and complex region relies on many generalizations for the abundant variations that are present, yet are not shown in our resultant bulk permeabilities. Our results do, however, provide a verification that there is relatively free movement of fluids within the layers between the seafloor and the Harbour Seam. This indication of high permeability occurring throughout the section provides strong evidence that the amount of fracturing occurring in the strata is much higher than expected. The preferred reason for such increases in fracturing are due to mining operations where the large sandstone units, which tend to be relatively well cemented, and fracture into blocks.

The accumulation of downward drawn water into layers above the mines, which tend to be composed of the higher permeable aquifer complexes (CBDC, 1994), is a major roof weighting concern. This accumulated water tends to create slumps of wall and roof material due to the zone of increased fracturing that surrounds the mining panel which tends to lower the structural integrity of the rock affected. Bulges in the slopes and faces of the mine walls, which also tend to cause serious weighting problems, are of concern as

well because they can greatly slow advancement in the panel because the material, mainly water, must be removed safely from the rock before the miners can continue. There is also general subsidence of the layers above the mine workings due to the removal of the coal seams. This kind of subsidence is also of major concern because as the rocks subside their permeabilities tend to increase drastically due to the large scale bed separation that is occurring directly above the panel.

The fracturing that occurs within the layers has been characterized as short, tight, and of high frequency (CBDC, 1994). The abundance of fracturing in these sections results in flow increases that occur along fracture surfaces and openings. The fracture zones are characterized by CBDC (1994) as having a bulk permeability range of 1×10^{-4} to 1×10^{-6} cm/sec. The application of this type of information to the overall formation clearly supports the range of bulk permeability that is achieved through the tidal lag method used in this thesis.

As the amount of fracturing increases due to bed separation, slumping and subsidence the permeabilities of all layers will increase. This is of concern because water is capable of passing through the formerly relatively low permeability layers in greater abundance as the amount of fracturing within layers increases.

The downward movement of once layered water-filled strata is of concern to the Phalen Colliery because, as the permeabilities continue to increase due to fracturing, the volume of water present above the Phalen Colliery will continue to increase. Therefore, the likelihood that water will flow into the workings in unmanageable quantities will depend largely on the stress-permeability characteristics of the rock that overlie the mine

workings. A deadly flow of water is classified by the CBDC as being a flow in excess of 7000 g.p.m. (31500 LPM). With the amount of water that entered the Lingan 2 east panel the CBDC took the right steps in trying to determine the cause of these water related problems by upgrading its monitoring system.

CHAPTER 6 CONCLUSIONS

6.1 Conclusions

Determination of bulk permeability within the Morien Group using ocean tidal forcing provides a comprehensive analytical method that indicates that the permeability of rocks overlying the Lingan Colliery can be calculated.

1. Using Darcy's Law for laminar flow the phase and amplitude shifts can be calculated and used to determine the permeability of the material through which the tidal signal travels.

2. The approach of using ocean tidal frequencies to generate a permeability result is an interesting way to apply theories such as Darcy's law. It has been determined that the range of hydraulic conductivity in the study area is 9.2×10^{-2} to 1.77×10^{-3} cm/sec and apparent permeability range is 1840.8 to 95680 mD.

3. In the strata between the Harbour seam and the seafloor there are multiple layers of sandstone, siltstone, mudstone, coal and some limestone, all of which show different permeability characteristics. As mining continues in the region the strata will continue to deform. These rocks are being placed under larger stresses than similar strata in a non-mining situation. This stress can cause fracturing in the layers with the lowest permeabilities. The abundance of small fractures is a key factor for the increase in

permeability within these rocks.

4. Chances of uncontrollable water inrushes into the Phalen mine are dependent on the stress distribution characteristics (fractures) of the material and changes in permeability in the section between the Phalen to Harbour seams.

5. Using the technique of this study it can be concluded that the vertical permeabilities found within the Sydney Mines Formation are high.

6. There are good reasons to continue monitoring water levels at the mines in the Sydney coalfield. Permeability increases close to the mine faces may increase the potential for water inrushes. Monitoring of the movement of the rocks above the mine could be used to model and predict the flow regimes and consequently inrush risk. Clearly, a well maintained and operated monitoring system that is concerned with the changing hydrostratigraphic characteristics of the mine is very important. Such as system will allow CBDC to better predict and avoid dangerous inrush situations in the mine.

References

Aston, T. and Singh, R. 1983. A reappraisal of investigations into strata permeability changes associated with longwall mining. ***International Journal of Mine Water***, Vol. 2, No.1.

Bai, M. and Elsworth, D. 1990. Some aspects of mining under aquifers in China. ***Mining Science and Technology***, Vol. 10. pp. 81-91.

Cain, P., Forrester D.J. and Cooper, R. 1994. Water inflows at Phalen Colliery in the Sydney coalfield and their relation to interaction of workings. *In:* Proceedings, ***5th International Mine Water Congress, Nottingham (U.K.), September 1994.***

Cape Breton Development Corporation, Phalen Colliery. 1994. Risk Assessment Report, Volume 1.

Cape Breton Development Corporation, Phalen Colliery. 1994. Risk Assessment Report, Volume 2.

Chapman, R.E. 1981. ***Geology and Water, an introduction to fluid mechanics for Geologists***. Martinus Nijhoff / Dr. W. Junk Publishers, The Hague.

Davis, E., Becker, K., Wang, K. and Carson, B. 1995. Long-term observations of pressure and temperature in Hole 892B, Cascadia Accretionary Prism. ***Proceedings of the Ocean Drilling Project Program, Scientific Results***, Vol. 146. pp. 299-311.

Dohler, G. 1996. Tides in Canadian Waters. Http://www.chshq.dfo.ca/chs_hq/nautpubl/XTRA.html.

Dooley, D. 1995. ***Oceanography***. West Publishing Company, USA.

Ferris, J. 1963. Cyclic Water-Level Fluctuations as a Basis for Determining Aquifer Transmissibility. ***Methods of Determining Permeability, Transmissibility and Drawdown***. Geological Survey Water-Supply Paper 1536-I. pp. 305- 318.

Ferris, J., Knowles, D., Brown, R., and Stallman, R. 1963. ***Theory of Aquifer Tests, Groundwater Hydraulics***. Geological Survey Water-Supply Paper 1536-E. pp. 80-91.

Fetter, C.W. 1994. ***Applied Hydrogeology, 3rd Edition***. Prentice-Hall, Inc., Englewood Cliffs, New Jersey.

Freeze, R.A. and Cherry, J.A. 1979. ***Groundwater***. Prentice-Hall, Inc., Englewood Cliffs, New Jersey.

Garritty, P. 1983. Water flow into undersea mine workings. ***International Journal of Mining Engineering***. pp. 237-251.

Gibling, M.R. and Bird, D.J. 1994. Late Carboniferous cyclotherms and alluvial paleovalleys in the Sydney basin, Nova Scotia. ***Geological Society of America Bulletin,*** Vol. 106. pp. 105-117.

Gibling, M.R., Boehner, R.C., and Rust, B.R. 1987. The Sydney Basin of Atlantic Canada: an Upper Paleozoic strike-slip basin in a collisional setting. *In:* Sedimentary basins and basin forming mechanisms. *Edited by:* C. Beaumont and A.J. Tankard. Canadian Society of Petroleum Geologists, Memoir 12.

Hacquebard, P.A. 1983. Geological development and economic evaluation for the Sydney coalbasin, Nova Scotia. *In:* Current research, part A, Geological Survey of Canada, Paper83-1A, pp. 71-81.

Hacquebard, P.A., Cameron, A.R. and Donaldson, J.R. 1965. A depositional study of the Harbour Seam, Sydney coalfield, Nova Scotia. ***Geological Survey of Canada, Department of Mines and Technical Surveys***, Paper 65-15.

Holla, L. and Buizen , M. 1990. Strata movement due to shallow longwall mining and the effect on ground permeability. AusIMM Proceedings. No.1. pp. 11-18.

King, L.H., and Maclean, B. 1976. Geology of the Scotian Shelf. Geological Survey of Canada, Paper, 74-31, 31p.

MacKillop, K. 1994. The application of consolidation results in a paleoceanographic study from the eastern equatorial Pacific Ocean. Msc. thesis, Technical University of Nova Scotia, Halifax, N.S.

Reddish, D., Yao, X., Benbia, A., Cain, P., and Forrester, D. 1994. Modelling of Caving over the Lingan and Phalen mines in the Sydney coalfield Cape Breton. *In* Proceedings ***5th International Mine Water Congress, Nottingham (U.K.),*** **September 1994.**

Rouleau, A., Archambault, G., Tremblay, D. and Gaudreault, M. 1994. The distribution of hydraulic head and conductivity around mine drifts. *In* Proceedings, ***5th***

International Mine Water Congress, Nottingham (U.K.) , September 1994. pp. 163-169.

Rust, B., Gibling, M., Best, M., Dilles, S. and Masson, A. 1987. A sedimentological overview of the coal-bearing Morien Group (Pennsylvanian), Sydney Basin, Nova Scotia, Canada. ***Canadian Journal of Earth Sciences,*** Vol 24. pp. 1869-1885.

Wang, K. and Davis, E. 1996. Theory for the propagation of tidally induced pore pressure variations in layered subseafloor formations. ***Journal of Geophysical Research***, Vol. 101. NO B5, pp. 11,483-11,495.

Whittaker, B.N., Singh, R.N., and Neate, C.J. 1978. Effect on longwall mining on ground permeability and subsurface drainage. ***Longwall Mining/Permeability and Drainage.*** Vol. 1. pp. 161-183.

Whitworth, K.R. 1982. Induced changes in permeability of coal measure strata as an indicator of the mechanics of rock deformation above a longwall coal face. (Source Unknown)

Van der Kamp, G. and Gale, J. 1983. Theory of earth tide and barometric effects in porous formations with compressible grains. ***Water Resources Research,*** Vol. 19, No.2. pp. 538-544.

Phase Shift

November 1994

Number	Tidal (hrs)	Lingan Mine (hrs)	Difference (hrs)	Difference (sec)
1	190	201	11	39600
2	247	259	12	43200
3	266	279	13	46800
4	341	350	9	32400
5	371	381	10	36000
6	446	458	12	43200
7	563	572	9	32400
8	600	611	11	39600
9	682	691	9	32400
10	702	712	10	36000

January 1995

Number	Tidal (hrs)	Lingan Mine (hrs)	Difference (hrs)	Difference (sec)
1	174	184	10	36000
2	193	204	11	39600
3	262	273	11	39600
4	266	279	13	46800
5	342	350	8	28800
6	402	414	12	43200

Phase Shift

June 1995

Number	Tidal (hrs)	Lingan Mine (hrs)	Difference (hrs)	Difference (sec)
1	058	069	11	39600
2	134	143	9	32400
3	169	180	11	39600
4	206	218	12	43200
5	231	242	11	39600
6	296	307	11	39600
7	350	360	10	36000
8	395	405	10	36000
9	483	492	9	32400
10	520	530	10	36000

July 1995

Number	Tidal (hrs)	Lingan Mine (hrs)	Difference (hrs)	Difference (sec)
1	406	415	9	32400
2	490	500	10	36000
3	526	538	12	43200
4	643	653	10	36000
5	680	689	9	32400
6	704	715	11	39600

Phase Shift

October 1995

Number	Tidal (hrs)	Lingan Mine (hrs)	Difference (hrs)	Difference (sec)
1	360	374	14	50400
2	390	400	10	36000
3	446	454	8	28800
4	521	530	9	32400
5	540	550	10	36000
6	631	640	9	32400
7	668	680	12	43200

November 1995

Number	Tidal (hrs)	Lingan Mine (hrs)	Difference (hrs)	Difference (sec)
1	111	120	9	32400
2	200	210	10	36000
3	310	320	10	36000
4	342	351	9	32400
5	392	400	8	28800
6	438	447	9	32400
7	474	482	8	28800
8	501	510	9	32400
9	554	563	9	32400
10	579	590	11	39600
11	648	658	10	36000
12	683	692	9	32400

Phase Shift

May 1996

Number	Tidal (hrs)	Lingan Mine (hrs)	Difference (hrs)	Difference (sec)
1	108	166	8	28800
2	266	274	8	28800
3	271	300	9	32400
4	380	388	8	28800
5	463	472	9	32400
6	514	521	7	25200
7	563	571	8	28800
8	601	610	9	32400

June 1996

Number	Tidal (hrs)	Lingan Mine (hrs)	Difference (hrs)	Difference (sec)
1	011	020	9	32400
2	141	150	9	32400
3	192	200	8	28800
4	291	300	9	32400
5	374	384	10	36000
6	502	513	11	39600
7	552	560	8	28800
8	603	612	9	32400

Phase Shift

July 1996

Number	Tidal (hrs)	Lingan Mine (hrs)	Difference (hrs)	Difference (sec)
1	119	128	9	32400
2	218	227	9	32400
3	441	450	9	32400
4	577	587	10	36000
5	603	611	8	28800
6	683	691	8	28800

September 1996

Number	Tidal (hrs)	Lingan Mine (hrs)	Difference (hrs)	Difference (sec)
1	220	230	10	36000
2	442	450	8	28800
3	470	480	10	36000
4	579	588	9	32400
5	602	610	8	28800
6	684	693	9	32400

Amplitude

November 1994

Number	Tidal (cm)	Lingan Mine (cm)	Difference (cm)
1	153.85	8.45	145.4
2	69.23	-2.33	71.56
3	134.61	15.43	119.18
4	103.85	16.20	87.65
5	38.45	3.10	35.35
6	73.07	23.10	49.97
7	138.45	1.50	136.95
8	119.23	7.55	111.68
9	53.85	8.53	45.32
10	142.30	28.53	113.77

January 1995

Number	Tidal (cm)	Lingan Mine (cm)	Difference (cm)
1	58.01	-4.65	62.66
2	120.06	2.00	28.02
3	30.02	2.00	28.02
4	80.04	23.25	56.79
5	86.71	24.80	61.91
6	136.74	3.10	133.64

Amplitude

June 1995

Number	Tidal (cm)	Lingan Mine (cm)	Difference (cm)
1	120.06	1.55	118.51
2	103.39	0.78	102.61
3	120.06	3.10	116.96
4	97.38	19.38	78.00
5	110.06	1.55	108.51
6	143.41	14.73	128.68
7	6.67	-3.10	9.77
8	130.07	0.00	130.07
9	120.06	13.95	106.11
10	106.72	-3.10	109.82

July 1995

Number	Tidal (cm)	Lingan Mine (cm)	Difference (cm)
1	111.51	19.38	92.13
2	88.44	10.08	78.36
3	107.66	24.80	82.86
4	107.66	13.95	93.71
5	107.66	22.48	85.18
6	126.89	6.98	119.91

Amplitude

October 1995

Number	Tidal (cm)	Lingan Mine (cm)	Difference (cm)
1	123.04	23.25	99.79
2	65.37	12.40	52.97
3	96.13	-2.33	98.46
4	123.04	-3.10	126.14
5	23.07	0.00	23.07
6	130.73	6.20	124.53
7	34.61	-15.50	50.11

November 1995

Number	Tidal (cm)	Lingan Mine (cm)	Difference (cm)
1	130.73	25.58	105.15
2	123.39	21.70	101.15
3	110.06	7.75	102.31
4	43.36	-8.83	51.89
5	53.36	-3.88	57.24
6	110.05	2.33	97.72
7	143.41	-1.55	144.96
8	140.07	10.85	129.22
9	3.34	6.98	-3.64
10	-10.01	-5.43	-4.58
11	136.74	30.32	106.51
12	113.39	10.85	102.54

Amplitude

May 1996

Number	Tidal (cm)	Lingan Mine (cm)	Difference (cm)
1	-6.67	-12.40	5.73
2	113.39	6.20	107.19
3	133.4	27.90	105.50
4	116.73	4.65	112.08
5	136.74	34.10	102.64
6	133.4	34.10	99.30
7	120.06	5.43	114.63
8	123.39	7.75	115.64

June 1996

Number	Tidal (cm)	Lingan Mine (cm)	Difference (cm)
1	0.00	0.78	-0.78
2	116.73	3.88	112.85
3	106.72	6.20	110.52
4	130.07	-3.88	133.95
5	23.35	-3.88	27.23
6	120.06	13.95	106.11
7	113.39	16.28	97.11
8	126.73	10.08	116.65

Amplitude

July 1996

Number	Tidal (cm)	Lingan Mine (cm)	Difference (cm)
1	133.4	6.20	127.20
2	130.07	5.43	124.64
3	133.4	3.88	129.52
4	113.39	10.85	102.54
5	116.73	2.33	144.40
6	13.34	-11.63	24.97

September 1996

Number	Tidal (cm)	Lingan Mine (cm)	Difference (cm)
1	36.69	2.33	34.36
2	36.69	-3.88	40.57
3	126.73	3.10	123.63
4	33.35	-5.58	38.93
5	16.68	-10.85	27.53
6	140.07	2.33	137.74

Number	Depth to water below SL (x) (cm)	Phase Shift (t) (seconds)	Velocity ($v= x/t$) (cm/sec)	Amplitude Shift (i)	Permeability ($k= v/i$) (cm/sec)
November 1994					
1	22050	39600	0.5568	145.40	3.8×10^{-3}
2	22030	43200	0.5099	71.56	7.1×10^{-3}
3	22011	46800	0.4703	119.18	3.9×10^{-3}
4	21893	32400	0.6757	87.65	7.7×10^{-3}
5	21825	36000	0.6063	35.35	1.7×10^{-2}
6	21685	43200	0.5019	49.97	1.0×10^{-2}
7	21434	32400	0.6615	136.95	4.8×10^{-3}
8	21360	39600	0.5394	111.68	4.8×10^{-3}
9	21214	32400	0.6548	45.32	1.4×10^{-2}
10	21160	36000	0.5878	113.77	5.2×10^{-3}
January 1995					
1	19723	36000	0.5479	62.66	8.74×10^{-3}
2	19745	39600	0.4986	28.02	5.41×10^{-3}
3	19659	39600	0.4964	28.02	1.77×10^{-3}
4	19673	46800	0.4204	56.79	7.40×10^{-3}
5	19661	28800	0.6827	61.91	1.10×10^{-2}
6	19582	43200	0.4533	133.64	3.39×10^{-3}
June 1995					
1	17254	39600	0.4357	118.51	3.68×10^{-3}
2	17217	32400	0.5314	102.61	5.18×10^{-3}
3	17172	39600	0.4336	116.96	3.71×10^{-3}
4	17172	43200	0.3975	78.00	5.09×10^{-3}
5	17154	39600	0.4332	108.51	3.99×10^{-3}

Number	Depth to water below SL (x) (cm)	Phase Shift (t) (seconds)	Velocity ($v=x/t$) (cm/sec)	Amplitude Shift (i)	Permeability ($k=v/i$) (cm/sec)
June 1995 (cont..)					
6	17105	39600	0.4319	128.68	3.35×10^{-3}
7	17081	36000	0.4745	9.77	5.88×10^{-3}
8	17052	36000	0.4737	130.07	3.64×10^{-3}
9	17009	32400	0.5249	106.11	4.95×10^{-3}
10	16992	36000	0.4720	109.82	4.29×10^{-3}
July 1995					
1	16668	32400	0.5144	92.13	5.58×10^{-3}
2	16614	36000	0.4615	78.36	5.89×10^{-3}
3	16605	43200	0.3844	82.86	4.64×10^{-3}
4	16561	36000	0.4600	93.71	4.91×10^{-3}
5	16545	32400	0.5107	85.18	5.99×10^{-3}
6	16531	39600	0.4174	119.91	3.48×10^{-3}
October 1995					
1	15996	50400	0.3174	99.79	2.18×10^{-3}
2	16017	36000	0.4449	52.97	8.39×10^{-3}
3	16013	28800	0.5560	98.46	5.65×10^{-3}
4	15997	32400	0.4937	126.14	3.52×10^{-3}
5	16000	36000	0.4444	23.07	1.92×10^{-2}
6	15994	32400	0.4936	124.53	3.69×10^{-3}
7	15974	43200	0.3698	50.11	7.38×10^{-3}
November 1995					
1	15962	32400	0.4927	105.15	4.69×10^{-3}
2	15956	36000	0.4432	101.15	4.38×10^{-3}

Number	Depth to water below SL (x) (cm)	Phase Shift (t) (seconds)	Velocity ($v= x/t$) (cm/sec)	Amplitude Shift (i)	Permeability ($k= v/i$) (cm/sec)
November 1995 (cont...)					
3	15954	36000	0.4432	102.31	4.33×10^{-3}
4	15944	32400	0.4921	51.89	8.27×10^{-3}
5	15927	28800	0.5530	57.24	9.66×10^{-3}
6	15939	32400	0.4919	97.72	5.03×10^{-3}
7	15928	28800	0.5530	144.96	3.82×10^{-3}
8	15922	32400	0.4914	129.22	3.81×10^{-3}
9	15918	32400	0.4913	-3.64	7.72×10^{-3}
10	15924	39600	0.4021	-4.58	2.60×10^{-2}
11	15913	36000	0.4420	106.51	4.15×10^{-3}
12	15911	32400	0.4911	102.54	4.79×10^{-3}
May 1996					
1	15189	28800	0.5274	5.73	9.20×10^{-2}
2	15175	28800	0.5269	107.19	4.92×10^{-3}
3	15167	32400	0.4681	105.50	4.38×10^{-3}
4	15163	28800	0.5265	112.08	4.69×10^{-3}
5	15165	32400	0.4681	102.64	4.56×10^{-3}
6	15146	25200	0.6010	99.30	6.05×10^{-3}
7	15170	28800	0.5267	114.63	4.61×10^{-3}
8	15156	32400	0.4678	115.64	4.05×10^{-3}
June 1996					
1	15146	32400	0.4675	-0.78	2.43×10^{-2}
2	15144	32400	0.4674	112.85	4.14×10^{-3}
3	15136	28800	0.5256	110.52	4.76×10^{-3}

Number	Depth to water below SL (x) (cm)	Phase Shift (t) (seconds)	Velocity ($v= x/t$) (cm/sec)	Amplitude Shift (i)	Permeability ($k= v/i$) (cm/sec)
June 1996 (cont...)					
4	15122	32400	0.4667	133.95	3.48×10^{-3}
5	15089	36000	0.4191	27.23	1.53×10^{-2}
6	15083	39600	0.3809	106.11	3.59×10^{-3}
7	15066	28800	0.5231	97.11	5.39×10^{-3}
8	15059	32400	0.4648	116.65	3.98×10^{-3}
July 1996					
1	15012	32400	0.4633	127.20	3.64×10^{-3}
2	15012	32400	0.4633	124.64	3.72×10^{-3}
3	14962	32400	0.4618	129.52	3.56×10^{-3}
4	14949	36000	0.4153	102.54	4.05×10^{-3}
5	14949	28800	0.5191	144.40	4.54×10^{-3}
6	14930	28800	0.5184	24.97	2.08×10^{-2}
September 1996					
1	14822	36000	0.4117	34.36	1.19×10^{-2}
2	14787	28800	0.5134	40.57	1.27×10^{-2}
3	14770	36000	0.4103	123.63	3.32×10^{-3}
4	14759	32400	0.4555	38.93	1.12×10^{-2}
5	14760	28800	0.5125	27.53	1.86×10^{-2}
6	14748	32400	0.4552	137.74	3.31×10^{-3}